The Astrophysical Journal, 754:44 (26pp), 2012 July 20 doi:10.1088/0004-637X/754/1/44

THE ASTRALUX LARGE M-DWARF MULTIPLICITY SURVEY*

Markus Janson[1,2,5], Felix Hormuth[2], Carolina Bergfors[2], Wolfgang Brandner[2], Stefan Hippler[2], Sebastian Daemgen[3], Natalia Kudryavtseva[2], Eva Schmalzl[4], Carolin Schnupp[2], and Thomas Henning[2]
[1] Department of Astrophysics, Princeton University, Princeton, USA; janson@astro.princeton.edu
[2] Max Planck Institute for Astronomy, Heidelberg, Germany
[3] European Southern Observatories, Garching, Germany
[4] Leiden Observatory, Leiden University, Leiden, Netherlands
Received 2012 March 10; accepted 2012 May 17; published 2012 July 3

ABSTRACT

We present the results of an extensive high-resolution imaging survey of M-dwarf multiplicity using the Lucky Imaging technique. The survey made use of the AstraLux Norte camera at the Calar Alto 2.2 m telescope and the AstraLux Sur camera at the ESO New Technology Telescope in order to cover nearly the full sky. In total, 761 stars were observed (701 M-type and 60 late K-type), among which 182 new and 37 previously known companions were detected in 205 systems. Most of the targets have been observed during two or more epochs, and could be confirmed as physical companions through common proper motion, often with orbital motion being confirmed in addition. After accounting for various bias effects, we find a total M-dwarf multiplicity fraction of 27% ± 3% within the AstraLux detection range of 0.″08–6″ (semimajor axes of ∼3–227 AU at a median distance of 30 pc). We examine various statistical multiplicity properties within the sample, such as the trend of multiplicity fraction with stellar mass and the semimajor axis distribution. The results indicate that M-dwarfs are largely consistent with constituting an intermediate step in a continuous distribution from higher-mass stars down to brown dwarfs. Along with other observational results in the literature, this provides further indications that stars and brown dwarfs may share a common formation mechanism, rather than being distinct populations.

Key words: binaries: general – stars: late-type – techniques: high angular resolution

Online-only material: color figures, machine-readable tables

1. INTRODUCTION

The multiplicity of stars is an important characteristic for understanding how they form and evolve. The fraction of multiple stars has implications for the typical architecture of stellar and planetary systems, monitoring their orbital characteristics yields information that would otherwise be unavailable, and their distribution in orbits and masses can yield insights into the formation process (e.g., Burgasser et al. 2007; Goodwin et al. 2007). One clear observational trend that has gradually emerged is that the fraction of stars that have stellar companions depends on the masses of those stars. For instance, within the population of Sun-like stars (FGK-type), less than half (∼46%; Raghavan et al. 2010) are multiple (although a previous well-known survey gave a larger value of up to ∼67%, see Duquennoy & Mayor 1991). By contrast, for more massive stars in the AB-type range, upward of 80% appear to be in multiples (Shatsky & Tokovinin 2002; Kouwenhoven et al. 2007; Peter et al. 2012). The trend of decreasing multiplicity from massive stars to solar-mass stars also continues down to lower masses. In the M0–M6 spectral-type range, multiplicity fractions of ∼26%–42% have been found (e.g., Fischer & Marcy 1992; Delfosse et al. 2004). For even later-type objects in the VLM range (very low mass stars and brown dwarfs), the multiplicity frequencies are as low as ∼10%–30% (e.g., Bouy et al. 2003; Close et al. 2003; Gizis et al. 2003; Joergens 2008).

A challenging factor in previous surveys for multiplicity in low-mass stars has been limited sample sizes of ∼100 stars or less. Part of the reason for this is that M-stars are altogether more poorly characterized than higher-mass stars; for instance, due to their low brightnesses, they are generally not included in the *Hipparcos* catalog (Perryman et al. 1997). Hence, well-characterized samples of M-dwarfs that are appropriate for statistical studies have been hard to come by. However, recently a number of efforts have been made in identifying and characterizing nearby M-dwarfs (e.g., Riaz et al. 2006; Reid et al. 2007; Lépine & Gaidos 2011), which has mitigated this situation. Following the publications of these studies, we have undertaken an extensive effort to study the multiplicity properties of nearby M-stars with high-resolution imaging. An intermediate study of 124 of these targets has been previously published (Bergfors et al. 2010). Here, we summarize the full sample of 761 individual stars and perform studies of statistical properties of various sub-samples.

A large sample of stars and a catalog of their binarity properties are relevant for a wide range of scientific purposes. For instance, the formation of VLM objects remains less well understood than for Sun-like stars. Although there are many indications that they may form as the low-mass tail of regular star formation (e.g., Luhman et al. 2005; Bourke et al. 2006), there have also been alternative mechanisms proposed for the formation of some or all of these objects (e.g., Reipurth & Clarke 2001; Goodwin & Whitworth 2007; Basu & Vorobyov 2012). For instance, Thies & Kroupa (2007) argue that the different binarity properties of stars and VLM objects is an indication for separate formation mechanisms of the two populations. Sun-like stars have separations that peak broadly at ∼30 AU, and a rather uniform distribution of mass ratios (e.g., Duquennoy &

* Based on observations collected at the European Southern Observatory, Chile, under observing programs 081.C-0314(A), 082.C-0053(A), and 084.C-0812(A), and on observations collected at the Centro Astronómico Hispano Alemán (CAHA) at Calar Alto, operated jointly by the Max-Planck Institute for Astronomy and the Instituto de Astrofísica de Andalucía (CSIC).
[5] Hubble Fellow.

Mayor 1991; Raghavan et al. 2010), whereas VLM objects have separations that peak narrowly at smaller separations (3–10 AU), and show a preference to nearly equal masses of the components (e.g., Burgasser et al. 2007). A key question, then, is whether the transition in binary properties from Sun-like stars to VLM objects proceeds smoothly over the intermediate range. A large M-dwarf sample is ideal for addressing this question. If any break or bimodality occurs over this range, this would imply that there are indeed two separate formation scenarios at play, whereas if the progression is fully continuous and monotonous, the opposite would be the natural conclusion.

Besides statistical issues, the individual detections, confirmations, and observational parameters of binaries are highly useful. For instance, continued orbital monitoring can yield simultaneous brightnesses and masses of the components (e.g., Delfosse et al. 2000; Zapatero Osorio et al. 2004; Bouy et al. 2004; Liu et al. 2008). Since our main sample from Riaz et al. (2006) is young, one of the implications of this is that the ages of individual systems can be inferred through isochronal analysis (e.g., Janson et al. 2007). Conversely, for the youngest systems and lowest masses, the theoretical mass–luminosity relationships (e.g., Burrows et al. 1997; Chabrier et al. 2000), which are increasingly uncertain under such conditions, can be better constrained (e.g., Hillenbrand & White 2004; Konopacky et al. 2010).

The paper will be structured as follows. In Section 2, we will describe the observations and data reduction procedure used for the survey. In Section 3, the determination of the photometric and astrometric properties of each detected binary pair is described, along with the determination of the corresponding underlying physical parameters of the individual components. This is followed by a discussion of sub-sample selection for statistical purposes in Section 4. Most of the binaries have been observed over two or more epochs, and the astrometric analysis of those cases is discussed in Section 5. The statistical analysis is described in Section 6 for the multiplicity fraction, and for the distribution of physical parameters in Section 7. Finally, we summarize our results in Section 8. Furthermore, individual notes for targets in the survey as well as a summary of background contaminants are provided in Appendices A and B.

2. OBSERVATIONS AND DATA REDUCTION

For all observations in this survey, we have used AstraLux Norte (Hormuth et al. 2008) at the Calar Alto 2.2 m telescope in Spain and AstraLux Sur (Hippler et al. 2009) at the ESO/NTT 3.5 m telescope on La Silla in Chile. The two AstraLux cameras are a near-identical twin pair of high-speed electron multiplying cameras developed for a wide range of high-resolution imaging purposes (e.g., Hormuth et al. 2007; Sicilia-Aguilar et al. 2008; Daemgen et al. 2009). This is achieved through a technique known as "Lucky Imaging" (Tubbs et al. 2002; Law et al. 2006), where a very large number of frames (∼10,000) of very short integration time (∼10 ms) are collected during an observation. In such a short time as 10 ms, each frame can be seen as capturing a frozen state of the wavefront distortion pattern imposed by the atmosphere. These states will be statistically distributed over a wide range of distortion severity, where in some cases, the wavefront will be particularly well preserved, so that the Strehl ratio will be high in these frames. By rejecting the majority of frames and using only the few percent of highest Strehl ratio, we can gain substantially in spatial resolution in this way, and achieve almost diffraction-limited images, at the cost of image depth.

Our total sample consists of 761 unique stars, of which 124 were presented in Bergfors et al. (2010). In this study, we present results for the full sample. In most cases where a companion candidate was found, multiple observations of the same system have been taken over a baseline that is useful for common proper-motion tests, so that physical companionship can be stringently tested in those cases. The targets were chosen primarily from the Riaz et al. (2006) sample (569 stars) and additionally from the Reid et al. (2007) sample (198 stars), and are summarized in Table 1. The spectroscopic distances in the table were adopted from Riaz et al. (2006; but corrected for binarity for binaries detected with AstraLux, see Section 4). The targets were selected directly from the above samples without additional constraints imposed, except for the AstraLux Sur targets, where only M-stars within 52 pc were observed. For statistical purposes, we have constructed homogenized subsamples within the existing data. We will discuss various subsamples that were selected for specific statistical investigations in Section 4. With most stars being observed in two filters (Sloan Digital Sky Survey i' and z') and many of the binaries being observed twice or more, our survey encompasses more than 1600 individual observations, each of ∼10–12 minutes extent in telescope time. In total, this corresponds to approximately 300 hr of observations, which have been performed between 2007 January and 2010 February.

The raw frames produced by the camera were reduced with the dedicated AstraLux pipeline (Hormuth et al. 2008), which makes the frame selection and recombination of frames, with a Drizzle algorithm to oversample the image and produce an output pixel scale of 23.3 mas pixel^{-1} for AstraLux Norte and 15.4 mas pixel^{-1} for AstraLux Sur. Flat field and bias corrections are applied prior to the drizzling. Individual frames were aligned based on the brightest pixel in the oversampled frames, and the 10% best frames were selected for producing the final image. The pixel scale as well as the orientation of true north were monitored by observing astrometric references during the nights, in particular the Trapezium (Köhler et al. 2008) whenever it was visible, and M15 (van der Marel et al. 2002) at any other time. The representative uncertainties for these quantities, determined using the IRAF *geomap* procedure, are ∼2 μas pixel^{-1} in pixel scale, which typically does not dominate the error in astrometric separation since the separations of the binaries in our survey are small, and ∼0.°3 in orientation angle, which often does dominate the error in position angle for the binary astrometry.

A sample of reduced images are shown in Figure 1. The separation and brightness contrast of each binary (as discussed in the following section) along with the AstraLux detection limit is shown in Figure 2.

3. PHOTOMETRY AND ASTROMETRY

The procedure for determining photometric and astrometric quantities was already described in Bergfors et al. (2010), here we summarize that procedure. The relevant quantities to be determined are the magnitude differences between primary and secondary within each pair in each detected multiple system in i' and z' for photometry, and the projected separation and position angle of the components in each pair for astrometry. For close binaries (∼1″ or less), this was done with point-spread function (PSF) fitting, using the reference PSF of a single star to iteratively create binary configurations that minimize the squared residuals of the fit. For wider binaries, we used Gaussian

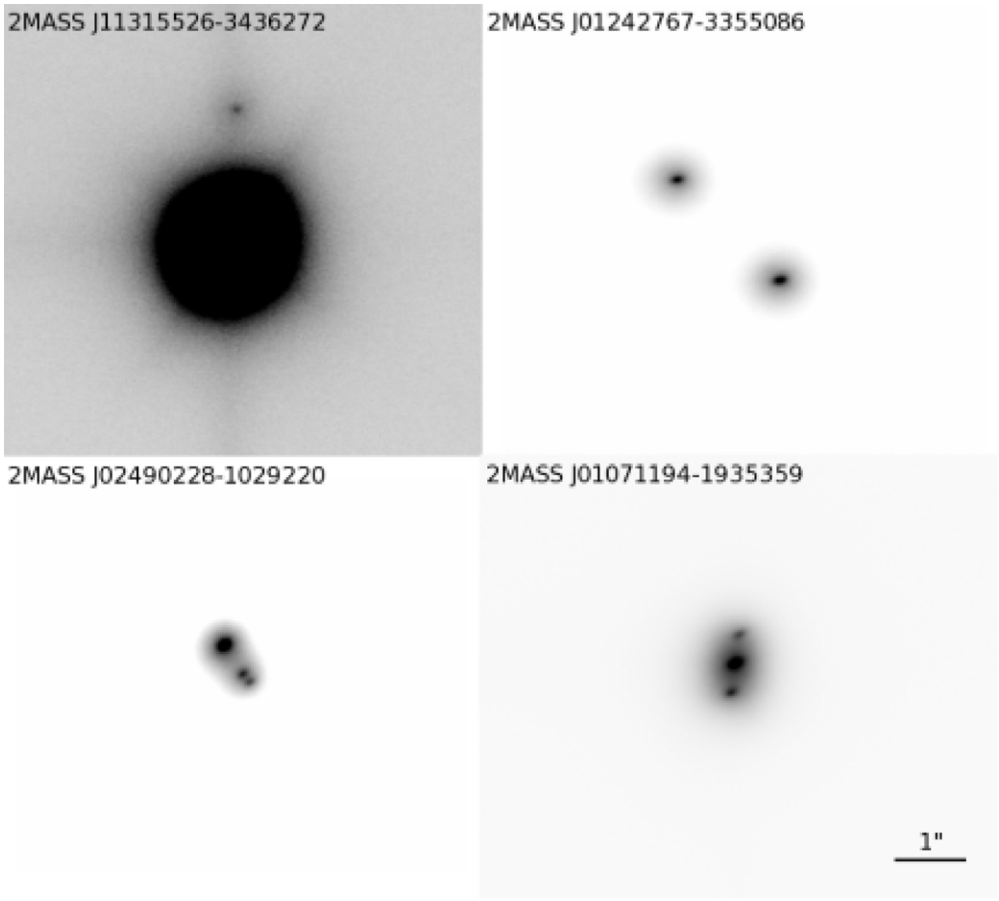

Figure 1. Four examples of multiple systems imaged in the AstraLux survey. Top left: a high-contrast binary. Top right: a low-contrast binary. Bottom left: a triple system. Bottom right: a binary displaying the fake triple effect, common for close low-contrast binaries. All images are in z', and in each case north is up and east is to the left.

Table 1
Properties of All Stars Observed in the AstraLux Campaign

2MASS ID	Other Name	SpT	D (pc)[a]	J (mag)	Mult.[b]	X-ray[c]	Sample[d]	Norte/Sur[e]
J00053484−0607070	LP 644-34	M2.5	25	9.28	S	N	IS	N
J00063925−0705354		M3.5	14	9.86	M	N	IS	N
J00080642+4757025		M4.0	12	8.55	S	Y	CS	N
J00142956+1331086		K7.0	70	9.34	S	Y	IS	N
J00150240−7250326		M1.0	41	8.62	M	Y	CS	S
J00155808−1636578		M4.0	9	8.74	S	Y	CS	S
J00165001−0710157		M0.0	64	9.58	S	Y	IS	N
J00171443−7032021		M0.5	48	9.00	S	Y	CS	S
J00193931+1951050		M4.0	23	10.93	S	N	IS	N
J00194303+1951117		M4.0	21	10.72	S	Y	CS	N

Notes.
[a] Distance is spectroscopic distance except for cases indicated by an acronym. Parallax distances: J52 (Jenkins et al. 1952), H80 (Harrington & Dahn 1980), A95 (van Altena et al. 1995), P97 (*Hipparcos*; Perryman et al. 1997), R02 (Reid & Cruz 2002), G04 (Gould & Chanamé 2000), R04 (Reid et al. 2004), H06 (Henry et al. 2006), L09 (Lépine et al. 2009), R10 (Reidel et al. 2010), and S10 (Smart et al. 2010). Kinematic distances: M05 (Mamajek 2005). The uncertainty in the spectroscopic distances is 37%.
[b] Multiplicity status as observed with AstraLux. M: multiple system. S: single star. BG: confirmed or suspected background star. U: unclear case.
[c] Flag for whether X-ray emission is detected at $>3.3\sigma$ (Y) or not (N), see Section 4 for details.
[d] This column lists membership of IS or CS (members of neither are marked with N). See Section 4 for details.
[e] Observed with AstraLux Norte (N) or Sur (S).

(This table is available in its entirety in a machine-readable form in the online journal. A portion is shown here for guidance regarding its form and content.)

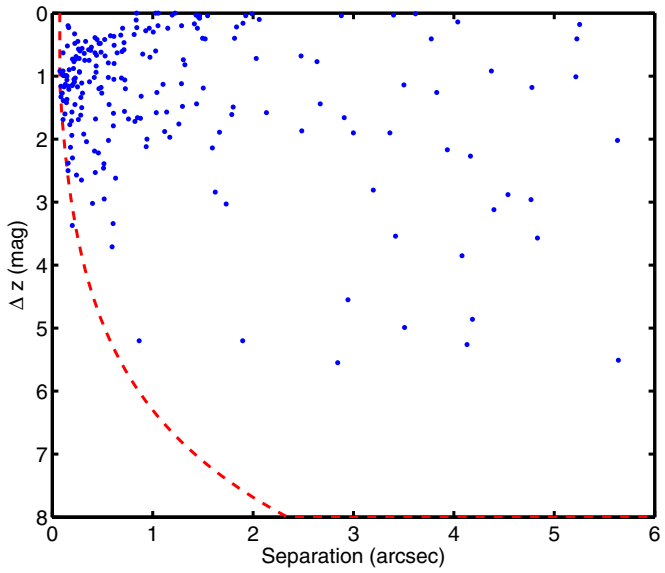

Figure 2. Separation and brightness difference in z' for all binary pairs detected with AstraLux, plotted along with the typical AstraLux detection limit. The small zone in the upper left that shows a lack of objects is likely due to a bias that tends to systematically overestimate the brightness difference for close pairs of nearly equal brightness.

(A color version of this figure is available in the online journal.)

centroid fitting of the primary and secondary in order to yield the photometric and astrometric parameters.

As is normally the case in Lucky Imaging data, some close and near-equal component binaries display the "fake triple" effect, where a ghost tertiary appears at the same separation from the primary as the real secondary, but on the opposite side of it. In these cases, we use the procedure of Law (2006) to "de-triple" the system, determining the true flux ratio of the binary components F_R as

$$F_R = \frac{2I_{13}}{I_{12}I_{13} + \sqrt{I_{12}^2 I_{13}^2 - 4I_{12}I_{13}}}, \quad (1)$$

where $I_{12} = F_1/F_2$ and $I_{13} = F_1/F_3$. When a fake triple occurs, or indeed more generally in any case of a close binary of nearly equal brightness, it is relevant to note that there can be a 180° phase ambiguity, given the difficulty to determine which star is actually the primary. This is especially true for such late-type stars as these, which are sometimes quite variable, such that the binary components alternate between which is the brightest. On this topic, it should be noted that because the brightness difference between the two components is taken as the apparently brighter component minus the apparently fainter one, it is a positive definite quantity. Hence, the measured brightness difference on, e.g., two equally bright components will not converge toward zero for a large number of measurements, since no measurement will be negative. This leads to a bias which exaggerates the brightness difference of close companions, and which most likely explains the apparent avoidance in the zone of very close binaries with almost equal-mass components (see Figure 2). The final photometry and astrometry values of each detected binary are listed in Table 2, and in Table 5 for the suspected or confirmed background contaminants.

In order to translate the integrated spectral type and relative photometry of each binary pair into individual spectral types and masses, we again follow the procedure in Bergfors et al. (2010), which was developed in Daemgen et al. (2007) and is based on the magnitude–spectral-type relationship in Kraus & Hillenbrand (2007). We base our final individual spectral types on the z' band, but we also make the same estimations on the basis of the i' band, which gives consistent spectral types to within ±0.5 sub-classes (except in those cases that have been identified as background objects). The translation of individual spectral types to component masses also follows the relations given in Kraus & Hillenbrand (2007). The resulting physical quantities for the pairs are listed in Table 3.

4. STATISTICAL SAMPLES

Out of our total sample, we construct two main sub-samples for the purpose of statistical analysis. This is done in order to remove statistical bias from selection effects and provide samples that are optimally suited for specific statistical studies. The first sample will be referred to as the inclusive sample (IS). This sample includes most of the stars observed, with some special cases excluded that are discussed toward the end of this section. However, this also includes 60 stars with estimated spectral types earlier than M-type (K7 and K5) that are additionally excluded in many of the statistical investigations.

The second sample is a sub-sample of the first and is called the constrained sample (CS). This sample is constructed to provide a multiplicity fraction that is well defined and bias free, following similar criteria to those in Bergfors et al. (2010). In CS, we make a cut for significant X-ray flux. This provides a sample that is young (less than ∼1 Gyr, see Bergfors et al. 2010) and provides further confirmation that the selected targets are indeed nearby M-dwarfs rather than misclassified distant objects, as can otherwise happen for these kinds of targets where a parallax is generally lacking. As in Bergfors et al. (2010), we use X-ray counts and errors from *ROSAT*[6] (Voges et al. 1999) with 3.3σ as the relevant significance criterion. In the case of binaries, this can lead to a selection effect due to the fact that the flux of the primary and secondary may add up to just above the significance criterion in cases where a single star would not have reached the criterion and thus not have been selected. We account for this in the same way as in Bergfors et al. (2010), by noting that L_X/L_{bol} is roughly constant as a function of spectral type, and calculating what the significance would have been for the primary component alone, had it been single. In those cases where the significance drops below the 3.3σ criterion, the binary is removed from the CS. These cases are labeled "S" in the X-ray column of Table 1.

We also adopt a 52 pc maximum distance cutoff for the CS, again analogously to Bergfors et al. (2010). However, in addition, we also take into account a further bias that favors selection of binaries. Since most of the distances are determined spectroscopically under the assumption that the primary is single, a system that is in reality a binary will appear artificially too bright for the primary spectral type, and thus appear closer than it really is. We correct for this by adjusting all the distances for binaries that do not have parallax measurements and are not resolved in the Two Micron All Sky Survey (2MASS) catalog (Skrutskie et al. 2006), which provided the brightness that the spectroscopic distance estimate was originally based on. Any binary that passes the 52 pc cutoff with the new distance estimate is removed from the CS. In the cases of both X-rays and distance, there can be stellar components inside of the resolution limit of

[6] Both the Bright Source Catalog IX/10A and the Faint Source extension IX/29.

Table 2
Relative Photometry and Astrometry of Confirmed and Unconfirmed Physical Pairs

2MASS ID	$\Delta z'$ (mag)	$\Delta i'$ (mag)	ρ ($''$)	θ (^{o})	Epoch	New
J00063925−0705354AB	1.17 ± 0.05	1.51 ± 0.01	0.250 ± 0.001	5.5 ± 0.4	2008.88	Y
J00150240−7250326AB	2.65 ± 0.03	2.72 ± 0.08	0.290 ± 0.009	69.1 ± 0.3	2008.86	Y
J00250428−3646176AB	3.34 ± 0.23	3.65 ± 0.21	0.605 ± 0.012	242.4 ± 0.3	2008.86	Y
J00325313−0434068AB	2.53 ± 0.06	3.17 ± 0.02	0.428 ± 0.006	179.2 ± 0.9	2008.88	Y
J00414141+4410530AB	0.36 ± 0.11	0.24 ± 0.07	0.579 ± 0.001	11.4 ± 0.3	2008.59	Y
J00485822+4435091AB	0.20 ± 0.11	0.17 ± 0.01	1.053 ± 0.002	254.2 ± 0.3	2008.59	N
J00503319+2449009AB	0.82 ± 0.04	0.90 ± 0.01	1.320 ± 0.001	319.0 ± 0.3	2008.59	Y
J01034210+4051158AB	0.68 ± 0.01	0.81 ± 0.01	2.477 ± 0.001	96.8 ± 0.3	2008.64	N
J01071194−1935359AB	0.63 ± 0.05	0.51 ± 0.02	0.426 ± 0.002	169.7 ± 0.3	2010.08	Y
J01093874−0710497AB	1.87 ± 0.03	2.01 ± 0.01	2.485 ± 0.015	75.9 ± 0.3	2008.64	Y
J01112542+1526214AB	1.11 ± 0.11	1.23 ± 0.10	0.293 ± 0.002	205.3 ± 0.3	2008.88	N
J01132817−3821024AB	0.17 ± 0.01	0.17 ± 0.01	1.415 ± 0.001	27.2 ± 0.3	2010.09	Y
J01132958−0738088AB	4.55 ± 0.08	5.18 ± 0.12	2.945 ± 0.007	227.63 ± 0.3	2007.85	Y
J01154885+4702259AB	0.93 ± 0.05	0.89 ± 0.10	0.271 ± 0.001	267.6 ± 0.4	2008.88	Y
J01210504−0402082AB	2.88 ± 0.18	3.14 ± 0.23	4.539 ± 0.001	137.2 ± 0.3	2008.64	Y
J01212520+2926143AB	0.57 ± 0.15	0.68 ± 0.10	0.260 ± 0.001	310.0 ± 0.3	2008.87	Y
J01242767−3355086AB	0.10 ± 0.01	0.07 ± 0.01	2.062 ± 0.002	43.2 ± 0.3	2010.08	N
J01433150+3904165AB	0.23 ± 0.83	0.20 ± 0.77	0.163 ± 0.004	273.8 ± 0.3	2008.88	Y
J01452133−3957204AB	2.00 ± 0.10	2.39 ± 0.16	0.943 ± 0.009	130.9 ± 0.3	2008.86	Y
J01483524−0955226AB	0.62 ± 0.18	0.68 ± 0.18	0.485 ± 0.001	154.2 ± 0.3	2008.87	Y
J01535076−1459503AB	0.04 ± 0.01	0.05 ± 0.01	2.879 ± 0.001	291.8 ± 0.3	2010.08	Y
J02002975−0239579AB	0.75 ± 0.06	0.89 ± 0.05	0.323 ± 0.001	5.9 ± 0.3	2008.87	Y
J02081218+1508424AB	0.01 ± 0.03	0.03 ± 0.03	3.617 ± 0.004	238.3 ± 0.3	2008.03	N
J02132062+3648506AB	2.13 ± 0.08	2.40 ± 0.10	0.181 ± 0.002	56.5 ± 2.2	2007.61	Y
J02133021−4654505AB	0.99 ± 0.02	0.79 ± 0.10	0.138 ± 0.005	96.4 ± 0.9	2010.11	Y
J02155892−0929121AB	2.62 ± 0.05	2.80 ± 0.05	0.631 ± 0.001	292.2 ± 0.3	2008.87	Y
J02155892−0929121AC	4.99 ± 0.05	5.52 ± 0.10	3.509 ± 0.002	299.3 ± 0.3	2008.87	Y
J02165488−2322133AB	0.92 ± 0.01	0.95 ± 0.01	4.374 ± 0.004	313.6 ± 0.3	2010.09	Y
J02255447+1746467AB	1.27 ± 0.05	1.17 ± 0.24	0.099 ± 0.001	278.4 ± 1.9	2008.87	Y
J02271603−2929263AB	1.49 ± 0.05	1.73 ± 0.03	1.801 ± 0.012	232.5 ± 0.3	2010.10	Y
J02335984−1811525AB	0.00 ± 0.01	0.00 ± 0.01	0.839 ± 0.006	49.0 ± 0.3	2010.09	Y
J02411909−5725185AB	1.19 ± 0.02	1.37 ± 0.01	1.504 ± 0.007	286.8 ± 0.3	2010.11	Y
J02451431−4344102AB	0.75 ± 0.03	0.84 ± 0.04	0.367 ± 0.001	184.4 ± 0.3	2010.09	Y
J02490228−1029220AB	1.27 ± 0.01	1.51 ± 0.03	0.493 ± 0.002	210.5 ± 0.3	2010.09	Y
J02490228−1029220BC	0.20 ± 0.04	0.29 ± 0.07	0.157 ± 0.001	217.4 ± 0.8	2010.09	Y
J02512559+1323125AB	3.85 ± 0.05	4.34 ± 0.05	4.081 ± 0.004	15.4 ± 0.3	2008.64	Y
J02545247−0709255AB	2.27 ± 0.03	2.52 ± 0.02	4.165 ± 0.011	285.3 ± 0.3	2010.09	Y
J02594789−0913109AB	3.71 ± 0.10	...	0.595 ± 0.008	319.9 ± 0.7	2008.88	Y
J03033668−2535329AB	1.72 ± 0.01	1.83 ± 0.01	0.823 ± 0.003	3.5 ± 0.3	2010.08	Y
J03042184+2118154AB	3.02 ± 0.07	2.92 ± 0.07	0.401 ± 0.001	300.0 ± 0.3	2008.64	Y
J03050976−3725058AB	1.03 ± 0.01	1.12 ± 0.05	0.229 ± 0.005	47.7 ± 0.3	2010.09	Y
J03323578+2843554AB	0.68 ± 0.03	0.79 ± 0.06	0.525 ± 0.001	106.4 ± 0.3	2008.88	Y
J03323578+2843554AC	2.38 ± 0.09	2.63 ± 0.17	0.158 ± 0.016	282.4 ± 2.0	2008.88	Y
J03415581−5542287AB	1.79 ± 0.05	2.16 ± 0.16	0.608 ± 0.004	262.5 ± 0.3	2010.10	Y
J03423180+1216225AB	5.20 ± 0.27	...	0.866 ± 0.008	17.8 ± 0.4	2008.87	Y
J03591438+8020019AB	2.30 ± 0.23	...	0.200 ± 0.006	356.7 ± 3.3	2009.01	Y
J04071148−2918342AB	1.92 ± 0.04	2.66 ± 0.13	0.313 ± 0.003	45.4 ± 0.3	2010.10	Y
J04080543−2731349AB	1.09 ± 0.06	1.40 ± 0.07	0.221 ± 0.003	216.7 ± 0.7	2010.09	Y
J04132663−0139211AB	1.68 ± 0.01	2.03 ± 0.04	0.759 ± 0.003	178.2 ± 0.3	2010.10	N
J04373746−0229282AB	1.34 ± 0.01	3.73 ± 0.01	0.284 ± 0.003	18.5 ± 0.6	2010.10	N
J04441107−7019247AB	0.77 ± 0.01	1.04 ± 0.01	2.636 ± 0.001	156.3 ± 0.3	2010.11	N
J04465175−1116476AB	0.40 ± 0.13	0.62 ± 0.16	1.497 ± 0.002	281.0 ± 0.3	2008.87	Y
J04595855−0333123AB	1.42 ± 0.05	1.55 ± 0.07	0.141 ± 0.001	302.7 ± 0.7	2010.08	Y
J05024924+7352143AB	1.27 ± 0.15	1.22 ± 0.05	0.301 ± 0.001	82.5 ± 0.3	2008.88	Y
J05100427−2340407AB	0.42 ± 0.01	0.45 ± 0.02	0.522 ± 0.001	128.3 ± 0.3	2010.08	Y
J05100488−2340148AB	0.40 ± 0.01	0.47 ± 0.01	1.815 ± 0.003	307.0 ± 0.3	2010.08	Y
J05115301−5246286AB	3.57 ± 0.05	4.52 ± 0.05	4.832 ± 0.012	36.3 ± 0.3	2010.09	Y
J05130132−7027418AB	1.89 ± 0.01	1.99 ± 0.01	1.665 ± 0.006	39.7 ± 0.3	2010.11	Y
J05191382−0059423AB	0.24 ± 0.15	0.23 ± 0.15	1.151 ± 0.002	211.6 ± 0.3	2008.87	Y
J05195412−0723359AB	0.58 ± 0.08	0.71 ± 0.08	0.714 ± 0.002	195.6 ± 0.3	2008.88	Y
J05195513−0723399AB	2.46 ± 0.07	2.68 ± 0.08	0.510 ± 0.002	303.9 ± 0.3	2008.88	Y
J05225705−0850119AB	0.35 ± 0.06	0.52 ± 0.07	0.682 ± 0.001	112.5 ± 0.3	2008.88	Y
J05234434−0753375AB	0.42 ± 0.20	0.36 ± 0.19	0.445 ± 0.005	189.1 ± 0.3	2008.88	Y
J05241914−1601153AB	0.37 ± 0.01	0.43 ± 0.03	0.613 ± 0.001	68.5 ± 0.3	2010.09	Y
J05254166−0909123AB	0.63 ± 0.01	0.69 ± 0.02	0.645 ± 0.001	54.9 ± 0.3	2010.09	N

Table 2
(Continued)

2MASS ID	$\Delta z'$ (mag)	$\Delta i'$ (mag)	ρ ($''$)	θ ($^{\circ}$)	Epoch	New
J05301858−5358483AB	0.73 ± 0.03	0.83 ± 0.02	0.232 ± 0.001	291.9 ± 0.3	2010.09	Y
J05301858−5358483AC	3.12 ± 0.02	3.45 ± 0.01	4.398 ± 0.009	327.7 ± 0.3	2010.09	Y
J05320450−0305291AB	1.05 ± 0.01	1.28 ± 0.02	0.216 ± 0.003	41.0 ± 1.1	2010.09	Y
J05343767−0543044AB	1.44 ± 0.03	1.74 ± 0.03	1.437 ± 0.001	267.4 ± 0.3	2008.87	Y
J05344858−3239362AB	1.58 ± 0.01	1.79 ± 0.01	2.133 ± 0.005	161.3 ± 0.3	2010.09	Y
J05344858−3239362BC	0.67 ± 0.01	0.80 ± 0.01	0.441 ± 0.001	186.6 ± 0.3	2010.09	Y
J05350429−0508125AB	5.26 ± 0.01	5.77 ± 0.01	4.131 ± 0.001	163.9 ± 0.3	2008.88	Y
J05355975−0616065AB	1.97 ± 0.01	2.33 ± 0.01	1.170 ± 0.001	17.0 ± 0.3	2008.88	Y
J05464932−0757427AB	5.55 ± 0.11	6.20 ± 0.12	2.843 ± 0.020	115.2 ± 0.3	2009.13	Y
J05494272−1158500AB	1.14 ± 0.02	1.16 ± 0.01	3.503 ± 0.007	110.2 ± 0.3	2010.08	Y
J06002304−4401217AB	0.04 ± 0.01	0.09 ± 0.01	1.927 ± 0.006	285.3 ± 0.3	2010.08	Y
J06012540−3225168AB	1.01 ± 0.01	1.11 ± 0.01	5.214 ± 0.005	16.1 ± 0.3	2010.09	Y
J06112997−7213388AB	1.21 ± 0.04	1.16 ± 0.08	0.164 ± 0.002	316.6 ± 0.3	2010.11	Y
J06134171−2815173AB	0.00 ± 0.01	0.07 ± 0.01	1.056 ± 0.003	359.1 ± 0.3	2010.11	Y
J06134539−2352077AB	1.37 ± 0.02	1.49 ± 0.04	0.145 ± 0.002	320.0 ± 0.5	2010.10	Y
J06161032−1320422AB	1.94 ± 0.12	1.40 ± 0.23	0.194 ± 0.008	170.6 ± 0.3	2008.87	Y
J06234024−7504327AB	1.45 ± 0.04	1.59 ± 0.06	0.566 ± 0.005	97.7 ± 0.3	2010.11	Y
J06262932−0739540AB	0.48 ± 0.11	0.49 ± 0.10	0.465 ± 0.002	84.6 ± 0.3	2008.88	Y
J06281861−0110504AB	0.03 ± 0.05	0.06 ± 0.02	1.432 ± 0.001	152.8 ± 0.3	2008.88	Y
J06351837+4745366AB	2.17 ± 0.06	2.26 ± 0.07	3.935 ± 0.003	264.9 ± 0.3	2008.88	Y
J06434532−6424396AB	0.94 ± 0.07	1.13 ± 0.03	0.271 ± 0.008	13.0 ± 0.6	2010.11	N
J06434532−6424396AC	2.12 ± 0.01	2.67 ± 0.01	0.935 ± 0.006	295.1 ± 0.3	2010.11	N
J06583980−2021526AB	0.24 ± 0.01	0.30 ± 0.01	1.445 ± 0.004	197.2 ± 0.3	2010.10	Y
J07102991−1637350AB	1.02 ± 0.01	0.92 ± 0.05	0.558 ± 0.003	355.1 ± 0.3	2010.09	Y
J07105990−5632596AB	1.88 ± 0.02	2.11 ± 0.02	1.119 ± 0.002	309.2 ± 0.3	2010.10	Y
J07115917−3510157AB	0.00 ± 0.01	0.11 ± 0.01	1.029 ± 0.006	32.9 ± 0.3	2010.09	Y
J07210894+6739590AB	1.77 ± 0.07	2.31 ± 0.03	0.174 ± 0.002	58.8 ± 1.2	2008.87	Y
J07223179+7305048AB	0.69 ± 0.28	0.92 ± 0.28	0.237 ± 0.002	195.3 ± 0.6	2008.87	Y
J07285137−3014490AB	1.20 ± 0.02	1.47 ± 0.03	0.464 ± 0.001	176.4 ± 0.3	2010.08	N
J07293108+3556003AB	1.15 ± 0.12	1.28 ± 0.08	0.198 ± 0.001	261.5 ± 0.3	2008.88	Y
J07313848+4557173AB	1.13 ± 0.04	1.41 ± 0.15	0.206 ± 0.001	353.0 ± 2.2	2009.13	Y
J07505369+4428181AB	0.72 ± 0.33	0.99 ± 0.23	2.031 ± 0.001	141.5 ± 0.3	2007.84	Y
J08031018+2022154AB	0.73 ± 0.19	0.88 ± 0.15	0.200 ± 0.002	48.4 ± 0.8	2009.13	Y
J08125835−1031581AB	1.44 ± 0.01	1.70 ± 0.01	2.669 ± 0.002	314.2 ± 0.3	2008.87	Y
J08224744−5726530AB	1.06 ± 0.01	1.17 ± 0.01	0.722 ± 0.003	137.5 ± 0.3	2010.09	Y
J08310177+4012115AB	0.16 ± 0.02	0.13 ± 0.02	1.899 ± 0.001	121.8 ± 0.3	2008.02	N
J08412528−5736021AB	0.08 ± 0.01	0.10 ± 0.01	1.467 ± 0.001	348.3 ± 0.3	2010.09	Y
J08445566−0637259AB	0.60 ± 0.14	0.65 ± 0.14	0.276 ± 0.007	22.0 ± 0.3	2008.87	Y
J08472263−4959574AB	0.22 ± 0.01	0.32 ± 0.01	1.835 ± 0.001	13.5 ± 0.3	2010.10	N
J08483696−1353087BC	0.58 ± 0.01	0.62 ± 0.00	0.362 ± 0.001	169.0 ± 0.3	2010.09	Y
J08540240−3051366AB	3.03 ± 0.02	3.28 ± 0.02	1.732 ± 0.010	157.3 ± 0.3	2010.09	N
J09053033−4918382AB	4.86 ± 0.06	5.50 ± 0.06	4.185 ± 0.012	258.7 ± 0.3	2010.08	Y
J09075823+2154111AB	0.92 ± 0.10	1.08 ± 0.09	0.107 ± 0.001	192.5 ± 1.1	2008.88	Y
J09164398−2447428AB	0.92 ± 0.07	0.90 ± 0.21	0.076 ± 0.012	160.5 ± 1.5	2010.08	Y
J09174473+4612246AB	0.45 ± 0.13	0.36 ± 0.12	0.254 ± 0.001	65.3 ± 0.6	2008.87	Y
J09180165−5452332AB	1.18 ± 0.02	1.18 ± 0.02	0.486 ± 0.001	83.1 ± 0.3	2010.08	Y
J09345604−7804193AB	1.68 ± 0.07	1.74 ± 0.06	0.431 ± 0.005	344.2 ± 0.3	2010.10	N
J09365782−2610111AB	0.54 ± 0.04	0.60 ± 0.03	0.389 ± 0.004	279.5 ± 0.8	2010.08	Y
J09423823−6229028AB	0.20 ± 0.01	0.30 ± 0.01	1.288 ± 0.004	264.0 ± 0.3	2010.10	Y
J10023100−2814280AB	2.02 ± 0.08	1.73 ± 0.09	0.559 ± 0.004	38.9 ± 0.3	2010.09	Y
J10122171−0128160AB	1.90 ± 0.02	1.97 ± 0.01	2.999 ± 0.007	291.2 ± 0.3	2010.09	Y
J10140807−7636327AB	1.45 ± 0.05	1.76 ± 0.05	0.226 ± 0.002	108.1 ± 0.5	2010.10	N
J10162867−0520320AB	2.81 ± 0.55	2.33 ± 0.32	3.198 ± 0.001	195.7 ± 0.3	2008.02	N
J10364483+1521394AB	1.26 ± 0.05	1.34 ± 0.04	1.042 ± 0.001	193.4 ± 0.3	2008.88	N
J10364483+1521394AC	1.32 ± 0.02	1.34 ± 0.14	0.885 ± 0.001	193.7 ± 0.3	2008.88	N
J10374401−0548577AB	2.39 ± 0.04	2.76 ± 0.13	0.514 ± 0.001	359.0 ± 0.3	2010.11	Y
J10394600+6545213AB	1.57 ± 0.04	1.63 ± 0.04	1.139 ± 0.002	320.6 ± 0.3	2008.87	Y
J11091380−3001398AB	0.94 ± 0.02	1.16 ± 0.02	0.436 ± 0.001	25.0 ± 0.3	2010.08	N
J11102788−3731520AB	0.41 ± 0.01	0.37 ± 0.01	1.523 ± 0.001	209.3 ± 0.3	2010.08	N
J11254754−4410267AB	...	0.88 ± 0.05	0.553 ± 0.003	259.7 ± 0.4	2010.08	Y
J11281625+3136017AB	1.13 ± 0.04	1.34 ± 0.05	1.103 ± 0.002	141.0 ± 0.3	2008.88	Y
J11315526−3436272AB	5.20 ± 0.04	6.93 ± 0.18	1.897 ± 0.011	354.6 ± 0.3	2010.11	N
J12062214−1314559AB	2.19 ± 0.04	2.46 ± 0.06	0.420 ± 0.003	64.9 ± 0.3	2010.11	Y
J1206557+700749AB	2.02 ± 0.05	2.03 ± 0.03	5.629 ± 0.007	60.3 ± 0.3	2009.42	N
J12134173−1122405AB	1.48 ± 0.06	1.71 ± 0.07	1.296 ± 0.002	269.1 ± 0.3	2009.13	Y

Table 2
(Continued)

2MASS ID	$\Delta z'$ (mag)	$\Delta i'$ (mag)	ρ ($''$)	θ (^{o})	Epoch	New
J12173945−6409418AB	0.18 ± 0.01	0.00 ± 0.05	5.252 ± 0.005	238.0 ± 0.3	2010.11	Y
J12173945−6409418AD	2.50 ± 0.03	...	0.157 ± 0.002	285.3 ± 6.9	2010.11	Y
J12173945−6409418BC	1.05 ± 0.01	1.87 ± 0.01	0.613 ± 0.001	317.9 ± 0.3	2010.11	Y
J12345629−4538075AB	0.51 ± 0.03	0.48 ± 0.02	0.616 ± 0.001	313.5 ± 0.3	2010.08	N
J12351726+1318054AB	0.45 ± 0.09	0.55 ± 0.10	0.332 ± 0.001	56.8 ± 0.3	2009.41	N
J12392104−5337579AB	0.06 ± 0.01	0.08 ± 0.01	1.455 ± 0.001	199.2 ± 0.3	2010.10	Y
J12545056+4048474AB	1.59 ± 0.34	1.79 ± 0.29	0.609 ± 0.001	32.7 ± 0.3	2009.41	Y
J12550001+3118248AB	0.47 ± 0.01	0.47 ± 0.01	0.714 ± 0.001	350.0 ± 0.3	2009.41	Y
J13013268+6337496AB	0.90 ± 0.27	...	0.168 ± 0.006	358.2 ± 0.8	2009.42	Y
J13015919+4241160AB	1.66 ± 0.07	1.89 ± 0.07	2.908 ± 0.008	247.9 ± 0.3	2009.42	Y
J13022691−5200507AB	1.33 ± 0.06	1.22 ± 0.06	0.085 ± 0.004	104.7 ± 1.1	2010.08	Y
J13022691−5200507AC	1.66 ± 0.02	1.74 ± 0.01	0.848 ± 0.008	247.1 ± 0.3	2010.08	Y
J13025257−5201384AB	0.48 ± 0.02	0.47 ± 0.06	0.478 ± 0.003	190.2 ± 0.3	2010.08	Y
J13061131+7025377AB	1.26 ± 0.01	1.36 ± 0.01	3.829 ± 0.001	102.4 ± 0.3	2009.42	Y
J13082484+3019094AB	0.88 ± 0.36	1.00 ± 0.41	0.210 ± 0.003	0.2 ± 0.6	2009.42	Y
J13120525+3213332AB	0.65 ± 0.17	0.98 ± 0.22	0.901 ± 0.002	227.0 ± 0.3	2009.41	Y
J13120689+3213179AB	1.16 ± 0.29	1.17 ± 0.11	0.161 ± 0.001	285.9 ± 1.2	2009.42	Y
J13151846−0249516AB	0.77 ± 0.23	1.20 ± 0.32	0.215 ± 0.002	201.5 ± 0.3	2009.13	Y
J13195689−6831142AB	1.67 ± 0.04	1.96 ± 0.03	0.878 ± 0.002	166.9 ± 0.3	2010.10	Y
J13293209+5142114AB	1.61 ± 0.02	1.98 ± 0.05	1.788 ± 0.001	303.9 ± 0.3	2009.42	Y
J13414631+5815197AB	0.79 ± 0.09	0.90 ± 0.08	0.558 ± 0.001	249.2 ± 0.3	2009.13	Y
J13493313−6818291AB	1.39 ± 0.20	1.50 ± 0.06	0.109 ± 0.016	240.7 ± 4.4	2010.10	Y
J13493313−6818291AC	1.12 ± 0.01	1.51 ± 0.01	1.286 ± 0.005	289.6 ± 0.3	2010.10	Y
J13534589+5210298AB	0.30 ± 0.02	0.15 ± 0.01	1.005 ± 0.002	343.9 ± 0.4	2008.64	Y
J13584500+3140179AB	0.99 ± 0.36	1.51 ± 0.36	0.122 ± 0.001	309.7 ± 2.9	2009.42	Y
J14360274+1334484AB	0.03 ± 0.03	0.04 ± 0.01	1.194 ± 0.002	48.5 ± 0.3	2009.42	Y
J14430789+1720463AB	2.96 ± 0.02	3.33 ± 0.03	4.768 ± 0.002	3.7 ± 0.3	2009.42	Y
J14433804−0414354AB	0.24 ± 0.02	0.27 ± 0.02	0.965 ± 0.001	287.7 ± 0.3	2008.45	Y
J15032251−0040310AB	0.41 ± 0.02	0.39 ± 0.02	3.775 ± 0.010	274.5 ± 0.3	2009.13	Y
J15280061+3431226AB	1.02 ± 0.08	0.96 ± 0.06	0.418 ± 0.002	322.0 ± 0.3	2009.42	Y
J15290296+4646240AB	0.72 ± 0.07	0.69 ± 0.16	0.268 ± 0.003	176.3 ± 0.3	2009.41	Y
J15312428+1900268AB	2.95 ± 0.07	3.39 ± 0.10	0.517 ± 0.001	283.2 ± 0.3	2009.42	Y
J15370409+3748275AB	1.62 ± 0.18	1.84 ± 0.09	0.283 ± 0.001	80.8 ± 0.4	2009.42	Y
J15553178+3512028AB	2.14 ± 0.04	2.21 ± 0.05	1.594 ± 0.003	257.5 ± 0.3	2008.45	N
J15594729+4403595AB	5.51 ± 0.12	6.33 ± 0.03	5.638 ± 0.004	284.8 ± 0.3	2009.42	Y
J16232165+6149149AB	0.59 ± 0.17	0.56 ± 0.19	0.382 ± 0.003	211.9 ± 0.6	2009.42	Y
J16291031+7804399AB	2.04 ± 0.04	1.25 ± 0.02	0.341 ± 0.002	6.1 ± 0.3	2009.42	Y
J16363309+6353452AB	3.37 ± 0.33	3.70 ± 0.21	0.199 ± 0.008	102.4 ± 0.4	2009.42	Y
J16363309+6353452AC	1.90 ± 0.02	2.23 ± 0.06	3.362 ± 0.005	198.3 ± 0.3	2009.42	N
J16411543+5344110AB	0.97 ± 0.04	0.73 ± 0.06	0.099 ± 0.005	94.4 ± 0.3	2009.42	Y
J16510995+3555071AB	1.58 ± 0.06	1.84 ± 0.13	1.035 ± 0.001	316.4 ± 0.3	2009.41	Y
J16552880−0820103AB	0.48 ± 0.11	0.55 ± 0.10	0.224 ± 0.002	81.0 ± 0.7	2009.42	N
J16590962+2058160AB	1.03 ± 0.10	1.22 ± 0.12	0.689 ± 0.001	139.0 ± 0.3	2009.42	Y
J17021204+5103284AB	0.34 ± 0.04	0.33 ± 0.01	0.816 ± 0.001	63.4 ± 0.3	2009.42	Y
J17035283+3211456AB	1.76 ± 0.03	1.93 ± 0.04	1.260 ± 0.001	142.6 ± 0.3	2009.41	N
J1724591+210838AB	0.03 ± 0.01	0.04 ± 0.01	3.399 ± 0.004	24.0 ± 0.3	2008.63	Y
J17250940−0633536AB	0.84 ± 0.12	1.07 ± 0.12	0.437 ± 0.001	283.5 ± 0.6	2009.42	Y
J17380077+3329457AB	0.60 ± 0.03	0.85 ± 0.05	1.029 ± 0.002	157.9 ± 0.3	2009.41	Y
J18110625+3543573AB	0.41 ± 0.01	0.61 ± 0.01	5.224 ± 0.008	26.2 ± 0.3	2009.41	Y
J18162484+5013570AB	0.24 ± 0.14	0.37 ± 0.07	0.701 ± 0.001	332.7 ± 0.3	2009.41	Y
J18464053−0916238AB	3.54 ± 0.27	3.95 ± 0.42	3.419 ± 0.003	266.6 ± 0.3	2008.45	Y
J18471129+2212413AB	1.09 ± 0.06	1.12 ± 0.03	0.371 ± 0.001	269.9 ± 0.4	2009.42	Y
J18592937−0403042AB	0.56 ± 0.10	0.72 ± 0.12	0.297 ± 0.002	137.5 ± 0.4	2009.42	Y
J19105480+3017476AB	1.69 ± 0.05	1.99 ± 0.13	0.259 ± 0.001	122.8 ± 0.4	2008.63	Y
J19105480+3017476AC	1.20 ± 0.09	1.42 ± 0.08	0.728 ± 0.001	65.2 ± 0.3	2008.63	Y
J19213210+4230520AB	1.60 ± 0.09	1.77 ± 0.11	0.126 ± 0.004	154.4 ± 0.3	2008.63	Y
J19224005−0612076AB	1.06 ± 0.18	1.52 ± 0.36	0.146 ± 0.001	79.9 ± 1.0	2009.42	Y
J19425324−4406278AB	...	1.39 ± 0.11	0.836 ± 0.002	349.8 ± 0.3	2008.87	Y
J19432464−3722108AB	2.84 ± 0.08	2.89 ± 0.07	1.623 ± 0.004	303.7 ± 0.3	2008.87	Y
J20003177+5921289AB	0.64 ± 0.24	0.69 ± 0.21	0.318 ± 0.002	267.3 ± 0.6	2009.41	Y
J20100002−2801410AB	0.80 ± 0.04	0.75 ± 0.03	0.615 ± 0.001	280.4 ± 0.3	2008.87	Y
J20163382−0711456AB	0.63 ± 0.15	...	0.107 ± 0.007	352.4 ± 2.1	2008.44	Y
J20500010−1154092AB	2.22 ± 0.21	2.61 ± 0.30	0.459 ± 0.007	350.3 ± 0.6	2008.63	Y
J20531465−0221218AB	1.16 ± 0.11	1.38 ± 0.13	0.086 ± 0.002	321.0 ± 8.0	2008.88	Y
J21035992+1218570AB	0.11 ± 0.03	0.12 ± 0.03	0.836 ± 0.005	70.0 ± 0.4	2009.42	Y

Table 2
(Continued)

2MASS ID	$\Delta z'$ (mag)	$\Delta i'$ (mag)	ρ ($''$)	θ ($^\circ$)	Epoch	New
J21091375−0814041AB	0.70 ± 0.01	0.94 ± 0.06	0.973 ± 0.002	120.4 ± 0.3	2008.88	Y
J21203506+3419476AB	0.99 ± 0.13	0.89 ± 0.14	0.109 ± 0.002	217.3 ± 1.3	2008.87	Y
J21205172−0301545AB	0.74 ± 0.05	0.82 ± 0.05	1.305 ± 0.002	69.7 ± 0.3	2008.63	Y
J21295166−0220070AB	1.56 ± 0.25	1.92 ± 0.36	0.719 ± 0.001	60.3 ± 0.3	2008.59	Y
J21365560−0840313AB	2.57 ± 0.36	3.44 ± 0.68	0.241 ± 0.008	109.0 ± 2.8	2008.59	Y
J21372900−0555082AB	0.33 ± 0.15	0.55 ± 0.09	0.222 ± 0.001	172.2 ± 0.3	2008.88	Y
J21422932+1233175AB	1.18 ± 0.14	1.37 ± 0.16	4.777 ± 0.003	8.9 ± 0.3	2007.84	Y
J22014336−0925139AB	0.28 ± 0.07	0.38 ± 0.08	0.930 ± 0.002	206.2 ± 0.3	2008.59	Y
J22232904+3227334AB	0.04 ± 0.02	0.05 ± 0.01	1.467 ± 0.001	234.9 ± 0.3	2009.42	N
J22240821+1728466AB	1.00 ± 0.14	1.16 ± 0.22	0.146 ± 0.007	208.8 ± 0.8	2009.42	Y
J22332264−0936537AB	0.04 ± 0.02	0.01 ± 0.02	1.547 ± 0.002	278.5 ± 0.3	2007.85	N
J22382974−6522423AB	0.23 ± 0.01	0.20 ± 0.02	0.842 ± 0.001	155.8 ± 0.3	2008.87	N
J22401867−4931045AB	0.14 ± 0.01	0.16 ± 0.01	4.039 ± 0.001	41.0 ± 0.3	2008.87	N
J22495622+1744414AB	1.17 ± 0.17	1.11 ± 0.26	0.117 ± 0.004	10.0 ± 0.7	2008.59	Y
J23062378+1236269AB	0.39 ± 0.09	0.49 ± 0.01	0.426 ± 0.001	316.9 ± 0.3	2008.59	N
J23172807+1936469AB	1.50 ± 0.12	1.70 ± 0.15	0.293 ± 0.001	19.2 ± 0.3	2008.59	N
J23261182+1700082AB	1.57 ± 0.09	1.90 ± 0.12	0.195 ± 0.002	51.8 ± 0.7	2008.63	Y
J23261707+2752034AB	0.52 ± 0.10	0.47 ± 0.10	0.151 ± 0.001	14.1 ± 0.3	2008.59	Y
J23450477+1458573AB	1.69 ± 0.05	1.76 ± 0.05	0.107 ± 0.004	177.5 ± 1.4	2008.59	Y
J23450477+1458573AC	0.00 ± 0.05	0.05 ± 0.05	1.222 ± 0.002	175.9 ± 0.3	2008.59	Y
J23495365+2427493AB	1.13 ± 0.04	1.23 ± 0.08	0.131 ± 0.001	324.6 ± 1.6	2008.88	Y
J23551649−0235417AB	0.61 ± 0.16	0.67 ± 0.08	0.694 ± 0.001	120.4 ± 0.3	2008.63	Y
J23570417−0337559AB	1.71 ± 0.05	2.06 ± 0.27	0.191 ± 0.001	282.4 ± 0.4	2008.88	Y
J23581366−1724338AB	0.01 ± 0.01	0.03 ± 0.01	1.989 ± 0.001	355.7 ± 0.3	2008.87	N

AstraLux which could have similar effects as those corrected for here. To first order, one might expect that such effects should affect singles and multiples within the AstraLux range of 0.″08–6.″0 equally, and thus not introduce any significant bias in the multiplicity fraction, although it should also be noted that some bias could be introduced if there is a strong correlation between the presence of a close companion and the presence of wider companions.

The CS also only contains primary stars in the spectral-type range of M0–M5. In contrast to the analysis in Bergfors et al. (2010), in this study we do not remove targets that are >6″ companions to stars of earlier spectral type than M0. The reason for this is that we are concerned with multiplicity in the range of 0.″08–6.″0, and so any companions or lack of companions beyond these limits should not be allowed to have an impact on the multiplicity statistics.

In total, 761 targets observed by AstraLux are presented here, of which 205 are multiple within 0.″08–6.″0. The IS sample contains 751 targets with K-stars (693 without K-stars), of which 203 (191 without K-stars) are multiple. The CS sample contains 337 targets, where 85 are multiple. The majority of the multiple systems are binary, but there are 12 triple systems and 1 quadruple system in the IS, and 6 triple systems in the CS (all within 0.″08–6.″0). These numbers include only those detected candidates that are consistent with common proper motion with the primary and/or the expected color–magnitude relationship of a physical companion, and not those that have been rejected in this regard (see Section 5 for details on the companionship analysis).

There are also 10 targets that are not included in either statistical sample. Seven of these were excluded because their multiplicity status is unclear. Since the resolution and contrast limits are not sharp cutoffs and since there is some variability in data quality, there inevitably exist limit-case tentative detections where binarity is plausible, but cannot be firmly established, for instance because the binary fitting does not converge, or there is a deemed risk of mix-up with some temporary PSF extension of non-astronomical origin. In our sample, these cases are J05323611−0523010, J15403153+1736554, J15530484+4457446, J21375368−0444383, J22581643−1104170, J23353509−0613302, and J23385413−1246184. Data under better conditions or with larger apertures are needed to confirm or reject those potential companions as astronomical objects. The remaining three cases that are not included in any of our sub-samples are binaries that contain a white dwarf (WD). These systems, J03324345−0855391, J10162867−0520320, and J16291031+7804399, are discussed further in the individual notes.

5. MULTI-EPOCH ANALYSIS

Most of the multiples observed with AstraLux have been detected in multiple epochs. Systems that were first discovered with AstraLux were generally observed over more than one epoch, and in addition, literature astrometry exists for some systems that had been previously discovered. In each case where multi-epoch astrometry exists, it becomes possible to stringently test physical companionship through common proper motion, as well as to examine whether significant orbital motion is taking place. Hence, we perform such analysis for all systems observed in more than one epoch. For each system, we acquire a proper motion for the primary from the literature, either from *Hipparcos* (where available), or otherwise from the PPMXL (Röser et al. 2010) or NOMAD[7] catalogs. Likewise, whenever parallax values are available (see Table 1), they are used in the analysis; in the remaining cases, a parallax is calculated based on the spectroscopic distance estimate. Two epochs of astrometry are then chosen for each star, and the change in position is compared to the change that would be expected for an unrelated static background object. If the relative motion deviates by more than 3σ

[7] Available from http://www.nofs.navy.mil/nomad/ or VizieR I/297

Table 3
Derived Parameters for Confirmed and Unconfirmed Physical Pairs

2MASS ID	SpT_A	SpT_B	m_A (M_{sun})	m_B (M_{sun})	Sep. (AU)	Per.[a] (yr)	Sample[b]
J00063925−0705354AB	M3.0	M4.5	0.290	0.175	3.5 ± 1.3	14	IS
J00150240−7250326AB	M1.0	M4.5	0.540	0.175	11.7 ± 4.4	63	CS
J00250428−3646176AB	M2.5	M6.0	0.355	0.120	17.4 ± 6.5	144	CS
J00325313−0434068AB	M3.5	M6.0	0.245	0.120	4.9 ± 1.8	25	IS
J00414141+4410530AB	M2.0	M2.5	0.420	0.355	45.5 ± 16.9	493	IS
J00485822+4435091AB	M3.0	M3.0	0.290	0.290	47.0 ± 17.5	598	IS
J00503319+2449009AB	M3.5	M4.5	0.245	0.175	15.8 ± 5.9	137	CS
J01034210+4051158AB	K7.0	M0.0	0.630	0.590	79.3 ± 2.0	904	IS
J01071194−1935359AB	M1.0	M2.0	0.540	0.420	16.0 ± 5.9	92	CS
J01093874−0710497AB	M1.0	M4.0	0.540	0.200	94.4 ± 9.2	1508	CS
J01112542+1526214AB	M5.0	M6.0	0.150	0.120	2.7 ± 1.0	12	CS
J01132817−3821024AB	M0.5	M1.0	0.565	0.540	71.4 ± 26.4	812	CS
J01132958−0738088AB	K7.0	M5.5	0.630	0.135	192.8 ± 71.3	4329	IS
J01154885+4702259AB	M4.0	M5.0	0.200	0.150	7.4 ± 2.7	48	IS
J01210504−0402082AB	M0.0	M4.5	0.590	0.175	331.3 ± 122.6	9751	IS
J01212520+2926143AB	M3.5	M4.0	0.245	0.200	7.8 ± 2.9	46	IS
J01242767−3355086AB	M4.0	M4.0	0.200	0.200	31.4 ± 11.6	393	CS
J01433150+3904165AB	M3.5	M3.5	0.245	0.245	10.5 ± 3.9	69	IS
J01452133−3957204AB	K7.5	M3.5	0.610	0.245	30.2 ± 2.2	254	IS
J01483524−0955226AB	M4.0	M4.5	0.200	0.175	10.3 ± 3.9	76	IS
J01535076−1459503AB	M3.0	M3.0	0.290	0.290	72.6 ± 26.9	1149	CS
J02002975−0239579AB	M3.5	M4.5	0.245	0.175	19.0 ± 7.0	181	IS
J02081218+1508424AB	M4.5	M4.5	0.175	0.175	43.4 ± 16.1	684	IS
J02132062+3648506AB	M4.5	M6.5	0.175	0.115	2.1 ± 0.7	8	CS
J02133021−4654505AB	M4.0	M5.0	0.200	0.150	2.1 ± 0.8	7	CS
J02155892−0929121AB	M2.5	M5.0	0.355	0.150	17.1 ± 6.4	141	CS
J02155892−0929121AC	M2.5	M8.0	0.355	0.102	94.7 ± 35.1	1928	CS
J02165488−2322133AB	M3.5	M4.5	0.245	0.175	175.0 ± 64.7	5052	CS
J02255447+1746467AB	M4.0	M5.0	0.200	0.150	3.9 ± 1.4	18	IS
J02271603−2929263AB	M3.5	M5.0	0.245	0.150	102.9 ± 38.1	2349	IS
J02335984−1811525AB	M3.0	M3.0	0.290	0.290	59.4 ± 21.9	850	IS
J02411909−5725185AB	M3.0	M4.5	0.290	0.175	78.2 ± 28.9	1434	IS
J02451431−4344102AB	M4.0	M4.5	0.200	0.175	3.2 ± 1.2	13	CS
J02490228−1029220AB	M1.5	M3.5	0.480	0.245	19.2 ± 7.1	140	CS
J02490228−1029220BC	M3.5	M3.5	0.245	0.245	6.1 ± 2.3	30	CS
J02512559+1323125AB	K7.0	M4.5	0.630	0.175	167.3 ± 61.9	3411	IS
J02545247−0709255AB	M3.0	M5.5	0.290	0.135	212.4 ± 78.6	6716	CS
J02594789−0913109AB	M4.5	M9.5	0.175	0.083	21.1 ± 7.8	270	IS
J03033668−2535329AB	M0.0	M3.5	0.590	0.245	32.1 ± 2.9	281	CS
J03042184+2118154AB	M1.0	M5.0	0.540	0.150	25.7 ± 9.5	222	IS
J03050976−3725058AB	M2.0	M3.5	0.420	0.245	12.1 ± 4.5	73	IS
J03323578+2843554AB	M4.0	M4.5	0.200	0.175	7.2 ± 2.6	45	IS
J03323578+2843554AC	M4.5	M5.5	0.175	0.135	2.2 ± 0.8	8	IS
J03415581−5542287AB	M4.5	M6.0	0.175	0.120	9.3 ± 3.4	74	CS
J03423180+1216225AB	M4.0	>L0	0.200	...	14.0 ± 5.1	166	CS
J03591438+8020019AB	M2.0	M5.0	0.420	0.150	12.5 ± 4.7	83	IS
J04071148−2918342AB	M0.0	M3.5	0.590	0.245	17.3 ± 6.4	111	IS
J04080543−2731349AB	M3.5	M4.5	0.245	0.175	11.1 ± 4.1	81	CS
J04132663−0139211AB	M4.0	M5.5	0.200	0.135	10.0 ± 3.7	77	CS
J04373746−0229282AB	M0.0	M3.0	0.590	0.290	7.4 ± 2.7	30	CS
J04441107−7019247AB	M1.5	M3.0	0.480	0.290	61.2 ± 22.6	772	CS
J04465175−1116476AB	M3.0	M3.5	0.290	0.245	25.4 ± 9.4	248	CS
J04595855−0333123AB	M4.0	M5.5	0.200	0.135	2.3 ± 0.8	9	CS
J05024924+7352143AB	K7.0	M1.5	0.630	0.480	24.5 ± 9.0	163	IS
J05100427−2340407AB	M3.0	M3.5	0.290	0.245	27.7 ± 10.2	282	IS
J05100488−2340148AB	M2.0	M2.5	0.420	0.355	96.8 ± 35.8	1530	CS
J05115301−5246286AB	M2.5	M6.0	0.355	0.120	227.1 ± 84.0	7023	IS
J05130132−7027418AB	M3.5	M5.5	0.245	0.135	59.5 ± 22.0	1053	CS
J05191382−0059423AB	M2.5	M3.0	0.355	0.290	47.9 ± 17.7	584	IS
J05195412−0723359AB	M4.0	M4.5	0.200	0.175	63.0 ± 23.3	1155	IS
J05195513−0723399AB	M1.0	M4.5	0.540	0.175	31.6 ± 11.7	297	IS
J05225705−0850119AB	M2.0	M2.5	0.420	0.355	60.9 ± 22.6	764	IS
J05234434−0753375AB	K7.0	K7.5	0.630	0.610	43.3 ± 15.9	362	IS
J05241914−1601153AB	M4.5	M5.0	0.175	0.150	6.4 ± 2.4	40	CS
J05254166−0909123AB	M3.5	M4.0	0.245	0.200	17.7 ± 6.6	158	CS

Table 3
(Continued)

2MASS ID	SpT_A	SpT_B	m_A (M_{sun})	m_B (M_{sun})	Sep. (AU)	Per.[a] (yr)	Sample[b]
J05301858−5358483AB	M3.0	M4.0	0.290	0.200	5.4 ± 2.0	25	CS
J05301858−5358483AC	M3.0	M6.0	0.290	0.120	101.2 ± 37.4	2249	CS
J05320450−0305291AB	M2.0	M3.5	0.420	0.245	5.6 ± 2.1	23	CS
J05343767−0543044AB	M2.5	M4.0	0.355	0.200	148.7 ± 55.0	3443	IS
J05344858−3239362AB	M2.5	M4.5	0.355	0.175	116.1 ± 43.0	2430	IS
J05344858−3239362BC	M4.5	M5.0	0.175	0.150	23.8 ± 8.8	288	IS
J05350429−0508125AB	K5.0	M5.5	0.700	0.135	185.9 ± 68.8	3923	IS
J05355975−0616065AB	K7.0	M2.5	0.630	0.355	148.9 ± 55.1	2589	IS
J05464932−0757427AB	M3.0	>L0	0.290	...	128.3 ± 47.4	3817	IS
J05494272−1158500AB	M3.0	M4.0	0.290	0.200	164.6 ± 60.9	4267	CS
J06002304−4401217AB	M4.0	M4.0	0.200	0.200	132.3 ± 48.9	3403	IS
J06012540−3225168AB	M3.5	M4.5	0.245	0.175	151.2 ± 55.9	4058	CS
J06112997−7213388AB	M4.0	M5.0	0.200	0.150	2.3 ± 0.8	8	CS
J06134171−2815173AB	M3.5	M3.5	0.245	0.245	61.2 ± 22.6	967	IS
J06134539−2352077AB	M3.5	M5.0	0.245	0.150	3.3 ± 1.2	13	CS
J06161032−1320422AB	M3.5	M5.0	0.245	0.150	6.5 ± 2.4	37	CS
J06234024−7504327AB	M3.5	M5.0	0.245	0.150	27.3 ± 10.1	321	CS
J06262932−0739540AB	M1.0	M2.0	0.540	0.420	38.2 ± 14.1	341	IS
J06281861−0110504AB	M2.0	M2.0	0.420	0.420	114.6 ± 42.4	1893	IS
J06351837+4745366AB	M1.5	M4.5	0.480	0.175	236.1 ± 87.4	6340	IS
J06434532−6424396AB	M3.0	M4.0	0.290	0.200	11.0 ± 4.1	74	CS
J06434532−6424396AC	M3.0	M5.0	0.290	0.150	38.3 ± 14.2	505	CS
J06583980−2021526AB	M4.0	M4.0	0.200	0.200	62.0 ± 23.0	1092	IS
J07102991−1637350AB	M2.5	M4.0	0.355	0.200	32.2 ± 11.9	347	IS
J07105990−5632596AB	M1.5	M4.0	0.480	0.200	63.1 ± 23.3	860	IS
J07115917−3510157AB	M3.0	M3.0	0.290	0.290	58.3 ± 21.5	827	IS
J07210894+6739590AB	M3.0	M5.0	0.290	0.150	5.1 ± 1.9	25	CS
J07223179+7305048AB	M4.0	M4.5	0.200	0.175	4.1 ± 1.5	19	IS
J07285137−3014490AB	M1.5	M3.5	0.480	0.245	7.4 ± 0.2	33	CS
J07293108+3556003AB	M1.0	M3.0	0.540	0.290	8.5 ± 3.1	38	CS
J07313848+4557173AB	M3.0	M4.0	0.290	0.200	10.8 ± 4.0	72	CS
J07505369+4428181AB	M1.5	M2.5	0.480	0.355	110.0 ± 40.7	1786	IS
J08031018+2022154AB	M3.0	M4.0	0.290	0.200	8.1 ± 2.9	47	CS
J08125835−1031581AB	M3.5	M5.0	0.245	0.150	99.1 ± 36.7	2220	IS
J08224744−5726530AB	M4.5	M5.5	0.175	0.135	6.8 ± 2.5	45	CS
J08310177+4012115AB	M3.0	M3.0	0.290	0.290	98.5 ± 36.4	1816	IS
J08412528−5736021AB	M3.0	M3.0	0.290	0.290	81.5 ± 30.1	1366	IS
J08445566−0637259AB	M3.0	M3.5	0.290	0.245	7.9 ± 2.9	43	IS
J08472263−4959574AB	M1.0	M1.5	0.540	0.480	89.1 ± 33.0	1178	IS
J08483696−1353087BC	M2.5	M3.5	0.355	0.245	20.0 ± 7.4	163	IS
J08540240−3051366AB	M4.0	M7.0	0.200	0.110	17.8 ± 6.6	191	CS
J09053033−4918382AB	M4.0	>L0	0.200	...	138.1 ± 51.1	5133	CS
J09075823+2154111AB	M2.0	M3.5	0.420	0.245	3.6 ± 1.3	12	IS
J09164398−2447428AB	M0.5	M2.5	0.565	0.355	3.6 ± 1.3	10	IS
J09174473+4612246AB	M1.5	M2.5	0.480	0.355	6.2 ± 2.3	24	CS
J09180165−5452332AB	M4.0	M5.0	0.200	0.150	7.3 ± 2.7	47	IS
J09345604−7804193AB	M3.0	M4.5	0.290	0.175	20.4 ± 7.6	191	CS
J09365782−2610111AB	M4.0	M4.5	0.200	0.175	12.3 ± 4.6	100	CS
J09423823−6229028AB	M3.5	M3.5	0.245	0.245	83.6 ± 31.0	1544	IS
J10023100−2814280AB	M4.0	M6.0	0.200	0.120	9.0 ± 3.3	68	CS
J10122171−0128160AB	M3.0	M5.0	0.290	0.150	133.3 ± 49.3	3282	CS
J10140807−7636327AB	M4.0	M5.5	0.200	0.135	3.6 ± 1.3	17	CS
J10162867−0520320AB	M0.0	WD	0.590	...	332.6 ± 123.1	11169	N
J10364483+1521394AB	M4.0	M5.0	0.200	0.150	8.4 ± 3.1	58	CS
J10364483+1521394AC	M4.0	M5.0	0.200	0.150	7.1 ± 2.6	45	CS
J10374401−0548577AB	M2.5	M5.0	0.355	0.150	24.3 ± 9.1	238	CS
J10394600+6545213AB	M1.5	M4.0	0.480	0.200	25.3 ± 9.3	218	CS
J11091380−3001398AB	M1.5	M3.0	0.480	0.290	17.0 ± 1.3	113	CS
J11102788−3731520AB	M4.0	M4.5	0.200	0.175	7.6 ± 0.9	48	CS
J11254754−4410267AB	M4.0	M4.5	0.200	0.175	12.0 ± 4.4	96	CS
J11281625+3136017AB	M3.0	M4.0	0.290	0.200	38.5 ± 14.2	483	IS
J11315526−3436272AB	M2.5	M9.0	0.355	0.088	83.5 ± 7.6	1621	CS
J12062214−1314559AB	M3.5	M5.5	0.245	0.135	11.2 ± 4.2	86	CS
J1206557+700749AB	M3.0	M5.0	0.290	0.150	112.6 ± 41.7	2548	CS
J12134173−1122405AB	M1.5	M3.5	0.480	0.245	108.9 ± 40.3	1888	IS

Table 3
(Continued)

2MASS ID	SpT_A	SpT_B	m_A (M_{sun})	m_B (M_{sun})	Sep. (AU)	Per.[a] (yr)	Sample[b]
J12173945−6409418AB	M3.0	M3.0	0.290	0.290	252.1 ± 93.3	7434	IS
J12173945−6409418AD	M3.0	M5.5	0.290	0.135	7.6 ± 2.8	45	IS
J12173945−6409418BC	M3.0	M4.0	0.290	0.200	29.4 ± 10.9	322	IS
J12345629−4538075AB	M2.5	M3.0	0.355	0.290	44.4 ± 5.6	521	IS
J12351726+1318054AB	M6.0	M6.5	0.120	0.115	7.2 ± 2.7	56	IS
J12392104−5337579AB	M2.5	M2.5	0.355	0.355	91.4 ± 33.8	1467	IS
J12545056+4048474AB	M1.5	M4.0	0.480	0.200	91.9 ± 34.0	1511	IS
J12550001+3118248AB	M2.0	M3.0	0.420	0.290	86.2 ± 31.8	1343	IS
J13013268+6337496AB	M3.5	M3.5	0.245	0.245	7.2 ± 2.6	39	CS
J13015919+4241160AB	M2.0	M4.0	0.420	0.200	372.1 ± 137.7	12893	IS
J13022691−5200507AB	M2.0	M4.0	0.420	0.200	4.4 ± 1.6	17	CS
J13022691−5200507AC	M2.0	M4.0	0.420	0.200	44.1 ± 16.3	526	CS
J13025257−5201384AB	M3.5	M4.0	0.245	0.200	28.2 ± 10.4	318	IS
J13061131+7025377AB	M3.5	M4.5	0.245	0.175	202.9 ± 75.1	6307	IS
J13082484+3019094AB	M1.5	M3.0	0.480	0.290	13.3 ± 4.9	78	IS
J13120525+3213332AB	M2.5	M3.5	0.355	0.245	39.2 ± 14.6	448	IS
J13120689+3213179AB	M5.0	M6.0	0.150	0.120	8.3 ± 3.1	65	IS
J13151846−0249516AB	M3.5	M4.5	0.245	0.175	7.1 ± 2.6	41	IS
J13195689−6831142AB	M1.5	M4.0	0.480	0.200	50.4 ± 18.6	614	IS
J13293209+5142114AB	K7.0	M2.0	0.630	0.420	178.2 ± 65.9	3283	IS
J13414631+5815197AB	M3.0	M4.0	0.290	0.200	19.0 ± 7.1	167	CS
J13493313−6818291AB	M2.0	M4.0	0.420	0.200	5.8 ± 2.1	25	IS
J13493313−6818291AC	M2.0	M3.5	0.420	0.245	68.2 ± 25.2	977	IS
J13534589+5210298AB	M3.5	M4.0	0.245	0.200	29.3 ± 10.9	336	IS
J13584500+3140179AB	M4.0	M5.0	0.200	0.150	3.7 ± 1.3	17	IS
J14360274+1334484AB	M2.5	M2.5	0.355	0.355	149.3 ± 55.2	3062	IS
J14430789+1720463AB	K5.0	M3.5	0.700	0.245	1836 ± 679	114431	IS
J14433804−0414354AB	M2.0	M2.5	0.420	0.355	62.1 ± 23.0	786	IS
J15032251−0040310AB	M0.5	M2.0	0.565	0.420	449.2 ± 166.2	13567	IS
J15280061+3431226AB	M4.5	M5.5	0.175	0.135	24.6 ± 9.1	310	IS
J15290296+4646240AB	M4.5	M5.0	0.175	0.150	5.7 ± 2.1	34	IS
J15312428+1900268AB	M2.5	M5.5	0.355	0.135	25.6 ± 9.5	262	IS
J15370409+3748275AB	M2.0	M4.0	0.420	0.200	18.8 ± 7.0	146	IS
J15553178+3512028AB	M4.0	M6.0	0.200	0.120	17.0 ± 6.3	175	CS
J15594729+4403595AB	M1.0	M8.0	0.540	0.102	197.3 ± 73.0	4892	CS
J16232165+6149149AB	M2.5	M3.5	0.355	0.245	25.9 ± 9.6	241	IS
J16291031+7804399AB	K7.0	WD	0.630	...	51.6 ± 19.1	660	N
J16363309+6353452AB	M2.0	M5.5	0.420	0.135	12.8 ± 4.7	87	IS
J16363309+6353452AC	M2.0	M4.5	0.420	0.175	215.2 ± 79.6	5788	IS
J16411543+5344110AB	M0.0	M2.5	0.590	0.355	7.1 ± 2.6	28	IS
J16510995+3555071AB	M4.0	M5.5	0.200	0.135	55.2 ± 20.4	1002	IS
J16552880−0820103AB	M2.0	M3.0	0.420	0.290	1.3 ± 0.1	2	CS
J16590962+2058160AB	M3.0	M4.0	0.290	0.200	17.9 ± 6.6	153	CS
J17021204+5103284AB	M0.5	M1.5	0.565	0.480	60.1 ± 22.2	645	IS
J17035283+3211456AB	M3.0	M5.0	0.290	0.150	26.2 ± 9.7	286	CS
J1724591+210838AB	M2.0	M2.0	0.420	0.420	95.2 ± 35.2	1433	IS
J17250940−0633536AB	M0.5	M2.5	0.565	0.355	27.4 ± 10.2	211	IS
J17380077+3329457AB	K7.0	K7.5	0.630	0.610	64.6 ± 23.8	659	IS
J18110625+3543573AB	M0.5	M2.0	0.565	0.420	323.9 ± 119.8	8307	IS
J18162484+5013570AB	M0.5	M1.5	0.565	0.480	65.9 ± 24.4	740	IS
J18464053−0916238AB	M0.0	M5.0	0.590	0.150	171.0 ± 63.3	3677	CS
J18471129+2212413AB	M3.5	M4.5	0.245	0.175	16.5 ± 1.4	146	CS
J18592937−0403042AB	K5.0	K7.5	0.700	0.610	37.9 ± 14.0	288	IS
J19105480+3017476AB	M1.5	M4.0	0.480	0.200	10.8 ± 4.0	61	IS
J19105480+3017476AC	M1.5	M3.5	0.480	0.245	30.6 ± 11.3	281	IS
J19213210+4230520AB	M2.0	M4.0	0.420	0.200	3.3 ± 1.2	11	CS
J19224005−0612076AB	M2.5	M4.0	0.355	0.200	12.2 ± 4.5	81	IS
J19425324−4406278AB	M3.5	M4.5	0.245	0.175	42.6 ± 15.7	607	CS
J19432464−3722108AB	M3.5	M6.0	0.245	0.120	52.1 ± 19.3	880	CS
J20003177+5921289AB	M4.0	M4.5	0.200	0.175	8.4 ± 3.1	56	CS
J20100002−2801410AB	M2.5	M3.5	0.355	0.245	19.5 ± 7.2	157	CS
J20163382−0711456AB	M0.0	M2.0	0.590	0.420	5.4 ± 2.0	18	IS
J20500010−1154092AB	M3.5	M4.5	0.245	0.175	18.5 ± 6.9	174	IS
J20531465−0221218AB	M3.0	M4.0	0.290	0.200	3.5 ± 1.3	13	IS
J21035992+1218570AB	M3.5	M3.5	0.245	0.245	118.8 ± 44.0	2616	IS

Table 3
(Continued)

2MASS ID	SpT_A	SpT_B	m_A (M_{sun})	m_B (M_{sun})	Sep. (AU)	Per.[a] (yr)	Sample[b]
J21091375−0814041AB	M1.5	M2.5	0.480	0.355	95.0 ± 35.1	1433	IS
J21203506+3419476AB	M3.5	M4.5	0.245	0.175	3.7 ± 1.3	16	IS
J21205172−0301545AB	M4.0	M4.5	0.200	0.175	22.5 ± 8.3	246	IS
J21295166−0220070AB	M0.0	M3.5	0.590	0.245	72.8 ± 26.9	961	IS
J21365560−0840313AB	K7.0	M3.5	0.630	0.245	20.7 ± 7.6	142	IS
J21372900−0555082AB	M3.0	M3.5	0.290	0.245	5.5 ± 2.1	25	IS
J21422932+1233175AB	M1.0	M3.0	0.540	0.290	573.2 ± 212.1	21305	IS
J22014336−0925139AB	M1.5	M2.0	0.480	0.420	73.1 ± 27.0	932	IS
J22232904+3227334AB	M3.0	M3.0	0.290	0.290	23.5 ± 2.1	212	CS
J22240821+1728466AB	M4.0	M5.0	0.200	0.150	3.3 ± 1.2	14	CS
J22332264−0936537AB	M2.5	M3.0	0.355	0.290	56.3 ± 20.9	744	CS
J22382974−6522423AB	M3.5	M3.5	0.245	0.245	12.6 ± 1.2	90	CS
J22401867−4931045AB	M5.5	M5.5	0.135	0.135	40.4 ± 14.9	699	IS
J22495622+1744414AB	M0.0	M3.0	0.590	0.290	9.7 ± 3.6	46	IS
J23062378+1236269AB	M0.5	M1.5	0.565	0.480	15.8 ± 2.7	87	CS
J23172807+1936469AB	M3.0	M4.5	0.290	0.175	6.3 ± 2.3	33	CS
J23261182+1700082AB	M4.5	M6.0	0.175	0.120	3.2 ± 1.2	15	IS
J23261707+2752034AB	M3.0	M3.5	0.290	0.245	4.6 ± 1.7	19	CS
J23450477+1458573AB	M1.0	M3.5	0.540	0.245	6.4 ± 2.3	26	IS
J23450477+1458573AC	M1.0	M1.0	0.540	0.540	72.1 ± 26.7	833	IS
J23495365+2427493AB	M3.5	M4.5	0.245	0.175	6.7 ± 2.4	38	CS
J23551649−0235417AB	M4.0	M4.5	0.200	0.175	9.5 ± 3.5	68	IS
J23570417−0337559AB	M4.0	M5.5	0.200	0.135	13.6 ± 5.1	123	IS
J23581366−1724338AB	M2.0	M2.0	0.420	0.420	78.6 ± 29.1	1075	CS

Notes.
[a] Estimated period based on the system mass and approximate semimajor axis. This should only be interpreted on an order-of-magnitude basis.
[b] IS denotes inclusive sample and CS denotes constrained sample, see Section 4. N means the star is in neither sample.

from the background hypothesis, then the binary is considered as a confirmed physical binary. If in addition there is a more than 3σ deviation from exact co-motion, then the binary is considered to display significant orbital motion, with some exceptions. These are the cases for which the estimated period is very large relative to the observed motion over the observational baseline. Although there can be a significant excess of orbital motion over expectation if the orbit is close to periastron or if the distance to the system is considerably smaller than the mean value, there is also good reason for caution in the event that the astrometric errors have been underestimated in those cases. Hence, we regard such cases as unconfirmed with respect to orbital motion.

The alternative case where there is a less than 3σ deviation from the background hypothesis is somewhat more complicated, because in that case there is an ambiguity between orbital motion and non-common proper motion—in principle, there can be orbital motion that happens to bring the companion in the same direction as it would have moved relative to the primary, if it had been a static background source. There are a few cases in our sample where this issue is genuinely very complicated; these are discussed in the individual notes. However, in most cases, there are two clear groups of objects with non-significant common proper motion: those for which the expected motion is simply small compared to the astrometric errors, which we treat as unconfirmed with regards to companionship, and those that display a clear motion consistent with the background hypothesis, which we regard as being cases of background alignment. We summarize these results in Table 4.

The vast majority of the systems examined do exhibit a common proper motion, which confirms that background contamination is rare and that most binaries in the total sample (including most of those that have only been observed in a single epoch) are real physically bound systems, as can also be statistically inferred simply from the fact that the frequency of detected companions increases rapidly with decreasing projected separation, rather than the other way around, as would be expected if background contaminants were dominant (Bergfors et al. 2010). Furthermore, the group of systems for which the color of the secondary is inconsistent with expectations for a physical companion provide an excellent match to the group of systems that are best consistent with the background hypothesis in the proper-motion analysis. Hence, we conclude that false positives can be distinguished from real physical systems in our data with a high accuracy. All cases for which no common proper motion could be established (either due to only a single epoch being available, or due to insufficient motion with respect to the astrometric errors between the epochs) are listed in the individual notes in Appendix A. In order to quantify the risk of biasing the multiplicity statistics through misclassification of background targets as physical companions and vice versa, we can note that only two of the systems that were classified through both their colors and their proper motion give conflicting conclusions between these two measurements (J03050976−3725058 and J06583980−2021526, see individual notes). Since 134 of the systems have been doubly tested in this regard, this means that 1.5% of the systems are problematic, such that in the remaining 85 system that have not yet been doubly tested, we can expect one additional such system, giving three in total. Assuming that all these three systems are misclassified gives, for instance, a potential impact on the multiplicity fraction among the 337 targets in the CS sample of approximately ±1%. Aside from being generous in this context given the fact that the two targets listed

Table 4
Pairs Observed Over Several Epochs

2MASS ID	ρ ($''$)	σ_ρ	θ (^{o})	σ_θ	Epoch	Ref.	PM[a] (mas yr^{-1})	CPM[b]	OM[c]
J00063925−0705354	0.230	0.006	6.5	0.5	2008.63	This paper	143	Y	Y
	0.250	0.001	5.5	0.4	2008.88	This paper			
J00325313−0434068	0.422	0.012	180.0	2.2	2008.63	This paper	168	Y	N
	0.428	0.006	179.2	0.9	2008.88	This paper			
J00414141+4410530	0.580	0.002	10.7	0.3	2008.03	This paper	50	Y	Y
	0.579	0.001	11.4	0.3	2008.59	This paper			
	0.567	0.002	12.2	0.3	2009.13	This paper			
J00485822+4435091	1.09	0.05	241.55	2.00	1997.9	McCarthy et al. (2001)	190	Y	Y
	1.050	0.004	254.1	0.3	2008.03	This paper			
	1.053	0.002	254.2	0.3	2008.59	This paper			
	1.049	0.004	255.0	0.3	2009.13	This paper			
J00503319+2449009	1.0	...	315	...	1960	Mason et al. (2001)	203	Y	Y
	2.080	0.032	316	1	1991.25	Perryman et al. (1997)			
	1.648	0.005	317.12	0.07	2002.64	Strigachev et al. (2004)			
	1.370	0.002	318.3	0.3	2007.61	This paper			
	1.353	0.001	318.6	0.3	2008.03	This paper			
	1.320	0.001	319.0	0.3	2008.59	This paper			
	1.305	0.002	318.9	0.3	2008.86	Bergfors et al. (2010)			

Notes.
[a] Total proper motion per year.
[b] Flag for common proper motion (yes or no). "U" refers to unclear cases.
[c] Flag for significant orbital motion (yes or no). "U" refers to unclear cases.
[d] A large number of observations exist in the literature; one example listed here (see individual notes).
[e] See individual note for J12351726+1318054.
[f] Not included in binary statistics; see individual note.
[g] Please note that footnotes d, e, and f, and references to Chauvin et al. (2010), Correia et al. (2006), Delorme et al. (2012), Farihi et al. (2005), Jao et al. (2003), Köhler (2001), and Morlet et al. (2002) occur only in the machine-readable form in the online journal.

(This table is available in its entirety in a machine-readable form in the online journal. A portion is shown here for guidance regarding its form and content.)

above are not even included in the CS, this is in any case smaller than the statistical error, as shown in Section 6, and we can thus assume that the impact of this potential bias is negligible.

We do not make any attempts at more detailed orbital modeling even for systems with several epochs of observations—additional AstraLux epochs are still being acquired, and a detailed orbital analysis based on those results will be the subject of a future publication.

6. MULTIPLICITY FRACTION

6.1. Total Multiplicity Fraction

We calculate the total multiplicity fraction of M0–M5-stars between $0\farcs08$ and $6\farcs0$ based on our CS sample. The fraction of detected multiples in the CS is $85/337 = 25.2\%$. However, in order to get the actual multiplicity fraction in the range of $0\farcs08$–$6\farcs0$, we have to account for the fact that the detectability is incomplete for faint companions at small separations. We do this by noting that detectability is essentially complete for all separations as long as $\Delta z' \leqslant 1.2$ mag is fulfilled, and that it is complete for the full contrast range as long as $\rho \geqslant 1''$ is fulfilled (see Figure 2). We then assume that the distribution of $\Delta z'$ is independent of separation, such that $N_{1,1}/N_{1,2} = N_{2,1}/N_{2,2}$ would hold true under full completeness, where $N_{1,1}$ is the number of binary pairs with $\Delta z' \leqslant 1.2$ mag and $\rho < 1''$, $N_{1,2}$ is the number with $\Delta z' \leqslant 1.2$ mag and $\rho \geqslant 1''$, and $N_{2,1}$ and $N_{2,2}$ are the corresponding cases with $\Delta z' > 1.2$ mag. In other words, we assume that in the narrow-separation range of $0\farcs08$–$1\farcs0$, the fraction of low-contrast companions ($\Delta z' \leqslant 1.2$ mag) to high-contrast companions ($\Delta z' \leqslant 1.2$ mag) is the same as is measured outside of $1''$. Hence, the number of missed companions is the difference between the ideal $N_{2,1}$ that fulfills the equality and the actual measured number. In this context, it should be noted that the assumption of $\Delta z'$ being independent of separation should be taken with some caution, as discussed in Section 7.

In this way, we find that 7.4 companions are missing in the data, such that the actual multiplicity fraction is $(85+7.4)/337 = 27.4 \pm 3.1\%$, where the error is based on Poissonian statistics. There is a remaining incompleteness to low-mass brown dwarfs; although we are sensitive to L0-type companions out to 52 pc, later-type companions fall below the sensitivity limits for the distant part of the sample. However, given that such companions are rare even for closer systems (only three >L0 companions exist in the entire observed sample, see Table 3), this is most likely a marginal effect. Hence, in summary, we conclude that the multiplicity fraction of M0–M5-stars within $0\farcs08$–$6\farcs0$ is $27\% \pm 3\%$.

As mentioned above, our observations and statistical studies are focused on acquiring multiplicity statistics within the separation range covered by AstraLux of $0\farcs08$–$6\farcs0$. However, in order to put this discussion in a broader context, we will briefly discuss the implications for the total multiplicity fraction, irrespective of separation. We do this by comparing the result to the multiplicity study by Fischer & Marcy (1992) (abbreviated as FM92), which studies the full separation range by combining radial velocity and imaging data. Our limits in angular separation at the median distance of the sample of 30 pc correspond to projected separations of 2.4–180 AU. We translate this into statistically relevant physical separations by applying the FM92 correction factor of 1.26, yielding physical limits of 3–227 AU.

Out of the 37 companions detected in FM92, 14 are either inside of 3 AU or outside of 227 AU. Henceforth, we will assume that the completeness within 3–227 AU is approximately the same as outside of this range in FM92; the estimated completeness values in FM92 largely support such an assumption, although the values for very large separation are highly uncertain. Under this assumption, we can hypothesize that in addition to the 85 companions that we detect within 3–227 AU in our CS sample, there additionally exist $85 * 14/37 = 32.2$ companions outside of these limits. Some of these will exist in systems that appear single in the AstraLux images, and thus form an additional multiple system, whereas others will exist in systems the are already binary within 3–227 AU, and thus not affect the total multiplicity fraction (but only the higher-order fraction). To which extent these additional companions affect the multiplicity statistics thus depends on to which extent close or wide companions are correlated or anti-correlated with companions in the intermediate separation range. For the purpose of this discussion, we assume that there is no correlation, such that exactly 27.4% of the additional components occur in systems that had already been identified as multiple. This leaves 23.4 companions that contribute to the total multiplicity fraction over all separations, which consequently comes out to 34.4%. By comparison, the total multiplicity fraction in FM92 is given as $42\% \pm 9\%$. Alternatively, we may recalculate the FM92 multiplicity within 3–227 AU under the same assumptions, by removing multiplicity components that are outside of these ranges. This gives a fraction of 28% within 3–227 AU in FM92. Hence, our data imply a slightly lower multiplicity fraction than FM92, but the values are consistent within the errors (under the given assumptions).

6.2. Multiplicity Dependence on Spectral Type

After having examined the multiplicity fraction of the full population of M0–M5-stars, we turn to studying the dependence of multiplicity fraction on spectral type within the sample. It is already well known that this fraction increases globally with increasing primary mass, since the multiplicity fraction is higher for Sun-like stars at 46%–67% (Duquennoy & Mayor 1991; Raghavan et al. 2010), yet higher for yet more massive stars at >70% (e.g., Shatsky & Tokovinin 2002; Mason et al. 2009), and lower for brown dwarfs at 10%–30% (e.g., Burgasser et al. 2003; Joergens 2008). Given our large sample and relatively large range in stellar masses, we can check how the multiplicity fraction evolves as function of primary mass self-consistently within the sample. In other words, if there are any discontinuities along the range as opposed to a smooth decline toward smaller masses, these could potentially be noticeable in the data. We use the IS M-dwarf sample for this purpose.

A plot of the multiplicity fraction as a function of spectral type is shown in Figure 3. The distribution is consistent with a uniform trend, and with random scatter from Poisson errors around the trend. For instance, although the fraction at spectral-type M0 is lower than the fraction at M2, this is not statistically significant. We show this by making a linear fit to the data. The best fit (shown in Figure 3) gives a χ^2 of 10.1, corresponding to a probability that it matches the underlying distribution of 52.6%. Hence, a monotonous trend is fully plausible given the data, and there is no valid motivation to infer any sub-structure in the general trend. Furthermore, the slope of the line is negative with increasing sub-class (i.e., decreasing mass), with a coefficient of -0.025 ± 0.013. Thus, at a marginal significance of 1.9σ, we can confirm the trend of multiplicity function with stellar mass, even within just the M-star spectral-type range.

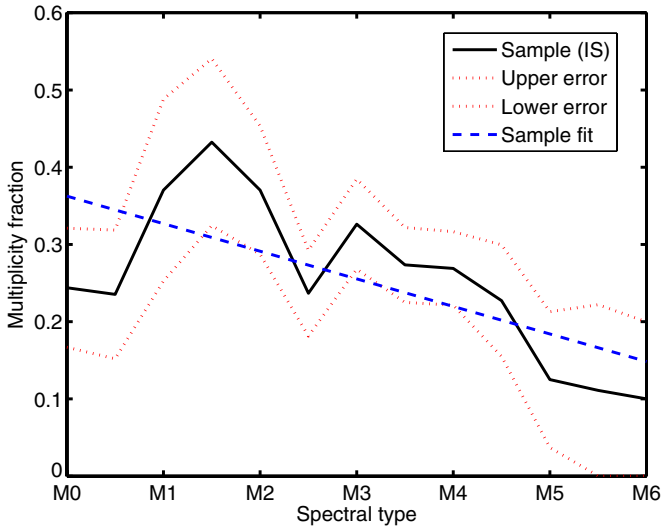

Figure 3. Multiplicity fraction as a function of primary spectral type. The data are consistent with a uniformly increasing trend with stellar mass.
(A color version of this figure is available in the online journal.)

7. PHYSICAL DISTRIBUTIONS

7.1. Distribution in Mass Ratio

The mass ratios of binaries among Sun-like stars and brown dwarfs have quite different distributions (e.g., Burgasser et al. 2007; Raghavan et al. 2010), where the mass ratios among Sun-like stars are quite uniformly distributed, while the components of brown dwarf binaries appear to be preferentially nearly equal in mass. It is thus interesting to study to whether M-dwarfs constitute a transitional regime between these two distributions, and if so, whether the transition is continuous or discrete. In order to demonstrate that this is a more complicated issue to address than it might seem at first, we first discuss the case of the IS sample.

A histogram of the mass ratios in the IS sample is shown in Figure 4. Here, the mass ratio is defined as $q_m = m_b/m_a$, where m_a is the primary mass and m_b is the secondary mass. The sample shown in the figure only includes binaries with separations larger than 1″, since smaller separations are subject both to bias due to the limited detectability of high-contrast systems in that range, as well as the high uncertainty in determining flux ratios of close binaries. The histogram shows a very pronounced peak at mass ratios near unity, in addition to a population with a more homogenous distribution. However, the peak is not physically real, as we can see if we plot the same distribution for the CS sample, shown in Figure 5. Again, this analysis contains only binaries with separations greater than 1″. For the CS sample, the distribution is much more homogenous, with no sharp peak near equal masses. The stark difference between the two samples can be easily understood by considering the biases that are involved. As we mentioned in Section 4, in the CS sample we have de-selected binaries that were positively selected for during observation preparations by appearing to be closer or brighter in X-rays than they would have been if they had been single. This effect is by far the strongest in binaries where the components have about equal brightness, and thus about equal mass. Hence, even though this is globally a subtle effect, in that the number of

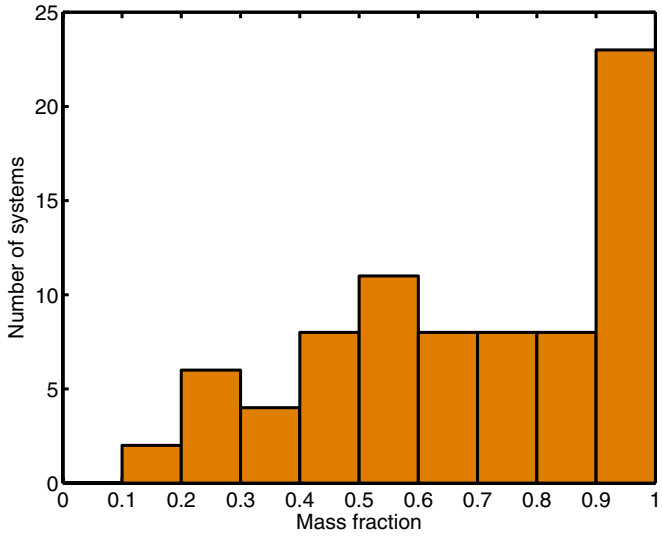

Figure 4. Histogram of mass ratios for the IS sample. The peak at near-equal masses is due to an observational bias, as explained in the text.

(A color version of this figure is available in the online journal.)

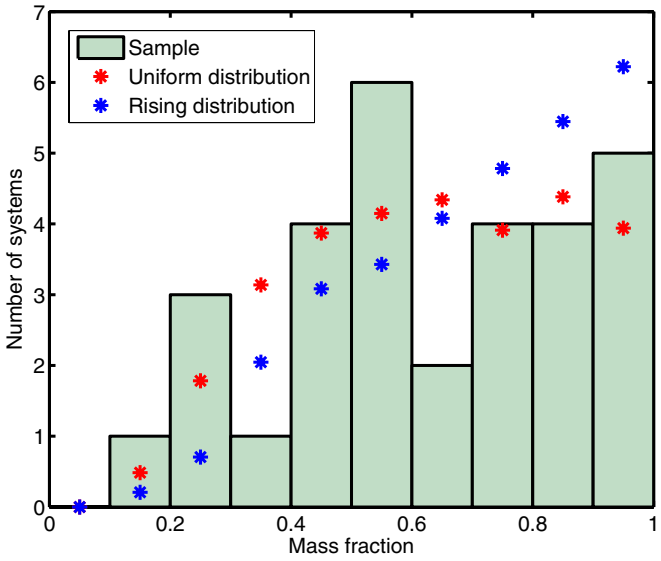

Figure 5. Histogram of mass ratios for the CS sample. Also plotted are the bias-corrected simulated distributions for the uniform and rising cases, normalized to the same number of total systems. The sample is better consistent with uniform distribution than a rising one.

(A color version of this figure is available in the online journal.)

binaries that are positively selected for is rather small compared to the total number of binaries and single stars in the survey, it is the case that in every event where it happens, the contaminating binary has a near-unity mass ratio and thus the effect becomes significant in the particular case of mass ratio investigations.

For this reason, we will concern ourselves only with the CS distribution for the rest of the mass ratio discussion. In order to examine this distribution in a bias-free manner, we need to take some observational effects into account. As a first step, we select only pairs with $>1''$ separations, as described above. In addition, we need to take into account the fact that the mass ratio in systems containing a brown dwarf candidate is highly uncertain, since brown dwarfs cool continuously after formation. Thus, the mass–luminosity relation depends on the highly uncertain age in those cases. We therefore remove all systems containing any component with a spectral type of L0 or later from our further analysis on the mass ratio distribution. However, this also introduces a bias (by preferentially removing systems with low-mass ratios) that needs to be accounted for. We do this by generating simulated populations and subjecting them to the same process, as described in the following.

As mentioned above, the most interesting scientific question regarding the mass ratio distribution concerns whether this distribution is best described as uniform, as for the Sun-like primary population, or as rising toward near-equal masses, as in the case of the brown dwarf population and as some star formation simulations predict should be the case also for low-mass stars (Bate 2012). We therefore generate simulated populations that follow these types of distribution. For each primary mass in our sample, 100 random mass ratios are generated. These are either uniformly distributed between zero and one (to represent the uniform case), or distributed between zero and one in such a way that the probability is directly proportional to the mass ratio (to represent the rising case). In every case where $q_{\rm m} * m_{\rm a} < 0.08\ M_{\rm sun}$, the system is removed from the analysis. The full population of all mass ratios for all stars is then compared to our observed sample using a Kolmogorov–Smirnov test (K-S test). Furthermore, this process is repeated 100 times performing the same test, in order to ensure that the result is statistically relevant. When assessing the probability that the two compared samples are drawn from the same distribution, we use the mean probability from the 100 tests. We find that the probability that our observed sample is consistent with a uniform distribution is 63.7%, but the probability for the rising distribution is only 8.9%. The simulated distributions are shown in Figure 5.

We also make the same comparison of a uniform and rising sample to the Bate (2012) sample of simulated star formation. In this case, we do not remove brown dwarfs since all samples are simulated and have no observational bias. As expected, the Bate (2012) sample provides a better match to the rising distribution with a probability of 39.4%, compared to the uniform distribution which has a probability of 11.1%. Hence, it follows that the mass distribution of our sample of M-stars is better described by a Sun-like uniform distribution, than by a distribution that moderately favors near-equal masses as in the Bate (2012) simulations, which one might have expected for an intermediate continuous population between Sun-like stars and brown dwarfs. This could imply that a sharp gradient or discontinuity occurs somewhere near the star/brown dwarf (BD) boundary, which would be difficult to consolidate with a common formation mechanism across this mass range. However, this issue should be considered with some caution, given the uncertainties in determining masses for brown dwarfs, as mentioned above. Also, it could for instance be the case that the mass ratio distribution depends on semimajor axis (e.g., Delfosse et al. 2004; Bate 2009). Here, we have studied a relatively wide population of binaries, since we removed $<1''$ binaries from the comparison. The mass ratio distribution of Sun-like stars is similarly dominated by wide binaries since their semimajor axis distribution peaks at such separations. By contrast, the brown dwarf population is dominated by small semimajor axes. A future specific study of M-dwarf multiplicity at small separations would be interesting in this regard (as well as an extensive survey of BD binarity at wide separations).

7.2. Distribution in Semimajor Axis

Since our survey has a typical inner semimajor axis cutoff at 3 AU which is somewhat comparable to the most interesting

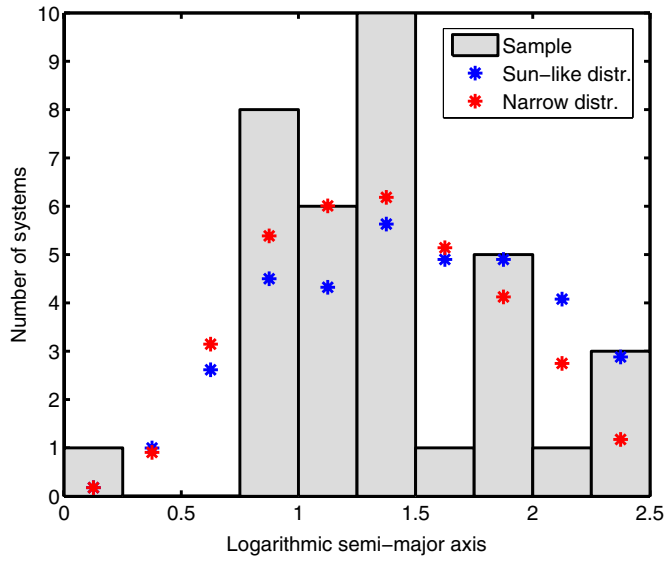

Figure 6. Histogram of semimajor axes for the CS sample. Also plotted is the bias-corrected simulated distribution for Sun-like stars, as well as a narrower distribution peaking at smaller separations. The sample is inconsistent with a Sun-like distribution, but better consistent with the narrower one.

(A color version of this figure is available in the online journal.)

region of distinction between the stellar and brown dwarf multiplicity populations at ∼10 AU, there is reason to proceed with care when determining this distribution in our sample. First of all, we use the CS sample for this purpose, in order to avoid distant targets that might skew the distribution. Also, we make a cut in flux ratio, keeping only binaries with $\Delta z' < 1.2$ mag, since there is a gradual loss of sensitivity to fainter companions inside of 1″, which could affect the apparent distribution. Furthermore, we include only stars with primary mass $>0.2\,M_{\rm sun}$, since lower-mass stars are not fully complete out to 52 pc and thus have smaller average distances than the full sample, which again could skew the distribution. These cuts leaves a sub-sample of a rather modest size, whose semimajor axis distribution is plotted in Figure 6.

The distribution appears to peak at smaller semimajor axes and be narrower than the corresponding distribution for Sun-like stars. In order to test this, we simulate binary populations with a Gaussian distribution in logarithmic semimajor axis space, with $\mu_{\rm sim} = 1.64$ and $\sigma_{\rm sim} = 1.52$ from Raghavan et al. (2010). For each star in our statistical sub-sample with a distance d, we generate 100 random semimajor axis values a following the above Gaussian distribution. In every case where $a/d/1.26 < 0\farcs08$ or $a/d/1.26 > 6\farcs0$, the simulated pair is removed from the analysis, in order to reproduce the existing bias in the observed population. The simulated population is then compared with the observed population using a K-S test, and this test is repeated 100 times in the same way as described in the previous section. This gives a 5.8% probability that the populations are drawn from the same distribution. As a reference case, we also repeat the same procedure for an example distribution with a lower mean and a narrower width ($\mu_{\rm sim} = 1.2$ and $\sigma_{\rm sim} = 0.8$), which gives a significantly higher probability of 55.5%. Hence, the results imply that M-dwarfs indeed have a semimajor axis distribution that is narrower and peaks at smaller values than for Sun-like stars. At the same time, the distribution seems to peak at larger separations than brown dwarfs, since it starts to drop already at ∼10 AU, which is probably not a bias-dominated trend, given that the median inner limit of detectability is 3 AU in our sample. This apparently intermediate distribution between Sun-like stars and brown dwarfs could be interpreted as another piece of evidence in favor of a common formation mechanism.

8. SUMMARY AND CONCLUSIONS

In this article, we have presented results for a high-resolution imaging survey of 761 low-mass stars with the AstraLux Norte and AstraLux Sur cameras, using the Lucky Imaging technique. We have detected 219 companions in 205 multiple systems, of which 182 companions in 171 systems were previously undiscovered. Our census of multiplicity in these young nearby M-stars is potentially useful for a wide range of future applications, such as calibration of theoretical isochrones for low-mass stars and determination of orbital distributions through continued orbital monitoring. The sample should also be useful for future planet-search projects, such as high-contrast imaging surveys, which typically seek to avoid close binaries as targets, or astrometry surveys with planned instruments such as GRAVITY (Eisenhauer et al. 2011), for which close binarity is highly desirable for astrometric referencing purposes.

Our sample also allows us to study the population statistics of M-dwarf binarity. We find that the multiplicity fraction of M0–M5-type stars between separations of 0.″08 and 6″ is 27% ± 3%. If we assume that close and wide binarity is uncorrelated with intermediate-range binarity, then this implies a total multiplicity fraction in the range of ∼34%, slightly lower than reported by Fischer & Marcy (1992) but consistent within the errors. Furthermore, we find that the multiplicity fraction as a function of primary mass in our sample is consistent with a smooth increase in multiplicity with increasing mass across the sample, as might be expected from the fact that the multiplicity is known to be higher for Sun-like stars and yet higher for high-mass stars, and lower for brown dwarfs. The mass ratios of the binary components in our sample on the other hand appear to be fully consistent with a uniform distribution and no preference toward near-equal masses. This is consistent with an equal distribution to Sun-like stars, which is distinct from the distribution of the brown dwarf population and may indicate a rather abrupt change in properties in the vicinity of the star–BD boundary. The semimajor axis distribution is however again consistent with a smooth intermediate stage between stars and brown dwarfs. Hence, the different multiplicity properties give conflicting information about whether or not the transition from stars to brown dwarfs is smooth, and thus whether or not they are best interpreted as sharing a common formation mechanism. On balance, given the two pieces of evidence in favor and the single one against, we consider a common mechanism to be more likely. We emphasize that no final conclusions can be based on these distributions alone, but that they should be interpreted as pieces of evidence in a larger picture, along with other lines of evidence from observations and simulations. Of course, it could also be the case that several different mechanisms are involved in the formation of brown dwarfs and VLM stars in overlapping mass ranges (e.g., Dupuy & Liu 2011; Riaz et al. 2012).

Most of the binaries and higher-order multiples in our sample have been observed at two or more epochs, which allows us to confirm common proper motion (as is expected for physical pairs but not for background contaminants) and to get a first handle on orbital motion. The vast majority of point sources in the AstraLux images are real physical companions, and the large difference in colors between companions and typical background stars allow us to distinguish between these two

cases, even for the targets that have only been observed in one epoch. Many of the targets show highly significant orbital motion and could have their complete orbital characteristics determined through further monitoring over a longer baseline.

An even more stringent and fully encompassing census of the multiplicity characteristics of this sample could be acquired through monitoring with radial velocity. This would allow us to discover binaries on smaller orbits, as well as to determine accurate mass ratios and various orbital elements of the binaries. In this way, many biases could be removed and a much larger fraction of the sample used for a wider range of statistical applications. We are already studying a subset of targets with this technique, and future spectrographs that are well suited for radial velocity at near-infrared wavelengths, such as CARMENES (Quirrenbach et al. 2010), should be able to further enhance such studies.

We thank all the staff at the Calar Alto and La Silla observatories for their support, and the referee, V. J. S. Béjar, for his useful report. This study made use of the CDS services SIMBAD and VizieR, as well as the SAO/NASA ADS service. Support for this work was provided by NASA through Hubble Fellowship grant HF-51290.01 awarded by the Space Telescope Science Institute, which is operated by the Association of Universities for Research in Astronomy, Inc., for NASA, under contract NAS 5-26555.

APPENDIX A

NOTES ON INDIVIDUAL BINARIES AND MULTIPLE SYSTEMS

Special remarks on individual systems are summarized below.

J00080642+4757025. In addition to the companion detected with AstraLux, J00080642+4757025 is a close spectroscopic binary with a 4.4 day period (Shkolnik et al. 2010), hence the system is actually a triple.

J00150240−7250326. The AstraLux PSF was strongly asymmetric for this target, hence in addition to the usual PSF fitting, we also performed a customized aperture photometry scheme in order to ensure that the PSF fitting did not provide a biased result. We chose a circular aperture with a three pixel radius centered on the primary and the companion, respectively. In order to estimate the influence of the primary PSF at the location of the secondary, we adopted the mean of aperture fluxes in two locations at the same separation as the secondary, azimuthally separated from it by ∼15 pixels in each direction. This mean value was subtracted from the aperture flux of the secondary, thus removing the influence of the stellar PSF. The results are well consistent with the PSF fitting values and the method seems more sensible for this particular type of application, hence we adopt the aperture photometry values for the differential photometry, and let the errors be represented by the scatter between PSF-fitting results and the aperture photometry. Note that the photometry values presented here should replace those in Bergfors et al. (2010).

J00193931+1951050. J00193931+1951050 and J00194303+1951117 are separated by only 53″, have very similar proper motions (e.g., Röser et al. 2010) and have similar estimated spectroscopic distances (23 and 21 pc, respectively) in Riaz et al. (2006), hence it is highly likely that they form a physical pair.

J00250428−3646176. Like J00150240−7250326, this stellar binary also had an asymmetric PSF, and we therefore calculated the photometry in the same way as for that case, see the individual note for J00150240−7250326. Note that the photometry values presented here should replace those in Bergfors et al. (2010).

J00424820+3532554. This system is noted as being triple in Tokovinin et al. (2006), including a close spectroscopic binary pair with approximately 1.3 mas separation and a likely wider companion at 11″ separation. Due to these separations however, it is counted as single for our purposes.

J00560596+4153282. The star has a likely companion at 13″ with similar proper motion (e.g., Röser et al. 2010) seen in 2MASS, but appears single closer in, in the AstraLux field of view.

J01034210+4051158. Aside from the companion seen in the AstraLux images, there is an additional possible wide companion at 26″ separation, as noted in the Washington Double Star (WDS) catalog (Mason et al. 2001). The wide components have very similar proper motions (e.g., Röser et al. 2010), so actual companionship seems probable.

J01093874−0710497. This binary displays clear common proper motion, but the residual astrometry does not seem to follow a simple trajectory consistent with only orbital motion of the two visible components. In addition, the brightness difference is larger than the spectral-type difference would imply at a common distance. This could indicate that the A component is itself an unresolved binary.

J01132817−3821024. The primary star in the system is a known eclipsing binary with a period of 0.4455 days (Parihar et al. 2009). Since the angular separation is inside of our inner cutoff, we count the system as a binary here for the purpose of multiplicity statistics, although it is really a triple system. To estimate the mass of the primary for the purpose of deriving the mass ratio to the tertiary component detected in our images, we use the sum of the masses corresponding to the individual spectral types, M1 and M3, derived for the eclipsing binary.

J01154885+4702259. In addition to the companion detected with AstraLux, it can be noted that J01154885+4702259 has a very similar proper motion to the star J01155017+4702023 at just 27″ separation (Röser et al. 2010), which is itself a close binary (Law et al. 2008). Thus, this is a very likely quadruple system.

J01452133−3957204. J01452133−3957204 has only been observed in one epoch, but the color and brightness of the detected companion are consistent with expectation, hence we count it as an unconfirmed binary.

J01473248+3453528. This star has a possible wide brown dwarf companion at 43″ separation, according to Casewell et al. (2008).

J01564714−0021127. This is an eclipsing binary with a 0.5 day period (Chen et al. 2006), but it is single in the AstraLux images.

J02002975−0239579. The companion to J02002975−0239579 has yet to be tested for common proper motion, but since its color and brightness are consistent with expectation and its separation is small (∼0.″32), it is counted as a physical companion here.

J02070176−4406380. J02070176−4406380 and J02070198−4406444 are separated by only 7″ and have similar estimated spectroscopic distances (13 and 21 pc, respectively) in Riaz et al. (2006), hence it is likely that they form a physical pair.

J02155892−0929121. This likely triple system has only been observed in one epoch, hence it remains unconfirmed.

The brightnesses and colors of all components are however consistent with expectation for a physical triple.

J02165488−2322133. The companion to J02165488−2322133 has not yet been confirmed to share a common proper motion, but the color and brightness of it are well consistent with a physical companion, hence it is counted as such in the statistics.

J02335984−1811525. There is insufficient motion between the two epochs of observation of J02335984−1811525 to establish common proper motion of the binary, but the components are nearly equal brightness and color, and reside at a relatively small separation of ∼0.″85, hence it is almost certainly a physical pair.

J02411909−5725185. J02411909−5725185 is yet to be confirmed as a common proper-motion binary, but the color and brightness of the companion are well consistent with it being physically bound, hence it is counted as a binary in the statistics.

J02411510−0432177. This star has been classified as a possible T Tau star in the Taurus–Auriga region by Li & Hu (1998).

J02451431−4344102. J02451431−4344102 is a member of an approximately equal-brightness binary with ∼50″ separation (Mason et al. 2001), in addition to being a close binary discovered with AstraLux.

J02490228−1029220. The system is precisely at the 3σ threshold for statistically significant exclusion of the background star hypothesis. By chance, the AB astrometry is just below the criterion (2.7σ) and BC is just above (3.1σ), so in principle the BC pair is inconsistent with chance alignment, if the pair does share a common proper motion with A. However, the proper motion of the system has of course been determined based on A, so until the AB physical connection has been demonstrated to the required accuracy, the 3.1σ confidence of the BC pair is irrelevant. Hence, we label the entire system as undetermined for now, although it is obviously very likely that the whole system is indeed bound.

J02545247−0709255. The primary is an SB2 binary with an 11.8 day period (Torres et al. 2002). Since the angular separation is inside of our inner cutoff, we count the system as a binary here (unconfirmed, since it has not yet been confirmed to share a common proper motion) for the purpose of multiplicity statistics, although it is really a triple system. To estimate the mass of the primary for the purpose of deriving the mass ratio to the tertiary component detected in our images, we adopt the mass ratio of 0.58 derived from the spectroscopic orbit and use the mass corresponding to an M3 spectral type for the primary.

J03032132−0805153. A possible wide companion to J03032132−0805153 at 172″ with similar proper motion is noted in WDS (Mason et al. 2001).

J03033668−2535329. One or both of the stars in this system must be highly variable. The magnitude differences between the primary and secondary vary from 5.14 mag to 1.72 mag between different observations in Bergfors et al. (2010) and here. In contrast to the individual note on this system in Bergfors et al. (2010), we assume here that the designation LTT 1453 refers to the primary star.

J03042184+2118154. The close (∼0.″40) companion to J03042184+2118154 is counted as an unconfirmed binary companion, since it has not yet been tested for common proper motion.

J03050976−3725058. This target, like J06583980−2021526, gives conflicting information about whether the AB pair is physically bound. The brightness and color are fully consistent with B being an M3.5 companion to the M2.0 primary. Furthermore, the separation is only 0.″2, and the whole field is otherwise empty. This indicates physical companionship. However, the deviation from the expectation of a background source is only 1.1σ, and the companion has moved 3.6 times closer to the background expectation than its original position where the motion has a 14σ confidence. This, by contrast, suggests a chance alignment. Since the magnitude of motion is not inconsistent with what could be expected for orbital motion of a real physical pair, we keep it as binary in our analysis, but we note that further observations will be necessary in order to resolve this issue satisfactorily.

J03283893−1537171. Also known as GJ 3228A, this star has a wide binary companion at 16″ separation (e.g., Weis 1991).

J03323578+2843554. This is a close triple system discovered with AstraLux, where in particular the tertiary component is difficult to fit for. Since the relative positions of the BC pair components are therefore clearly dominated by noise scatter in both separation and position angle, we set the error of each epoch to the scatter among the data points and make no assessment of orbital motion for the BC pair (although by contrast, clear orbital motion is seen of the pair with respect to the A component).

J03324345−0855391. J03324345−0855391 is a component in a system with a rather complex history, as it is a spectroscopic binary with a DA white dwarf with a 0.2 day period and has undergone a common envelope phase in the past (e.g., Davis et al. 2010). Hence, it cannot count as a regular M-star and is not included in the statistical analysis.

J03360868+3118398. This star has been classified as a possible T Tau star in the Taurus–Auriga region by Li & Hu (1998).

J03394784+3328306. Also known as GJ 9119 B, this star is a wide companion to GJ 9119 A at about 14″ as noted in, e.g., the WDS catalog (Mason et al. 2001). It is however single in the separation range covered by the AstraLux data.

J03415581−5542287. J03415581−5542287 and J03415608−5542408 are separated by only 12″ and have similar estimated spectroscopic distances (14 and 20 pc, respectively) in Riaz et al. (2006), hence it is likely that they form a physical pair. J03415581−5542287 is a close (∼0.″61) binary in our data, so the system is likely triple in reality, although common proper motion of all components has yet to be proven.

J03423180+1216225. Since the two epochs of observation were acquired over a baseline of only a few months, there is not yet sufficient motion to confirm common proper motion of the companion that was detected with AstraLux. However, the separation between the components is rather small (∼0.″86), and the fact that the companion is clearly detected in z' but too faint in i' implies that it must be very red, as expected for a real companion. Hence, we count it as a binary system for statistical purposes.

J03461399+1709176. This star has a possible wide companion at about 8″ as noted in, e.g., the WDS catalog (Mason et al. 2001). It is however single in the separation range covered by the AstraLux data.

J03472333−0158195. López-Santiago et al. (2006) classify this star as a member of subgroup B4 (a nearby young moving group), with an estimated age of ∼100 Myr.

J03591438+8020019. A companion to J03591438+8020019 was detected on two separate occasions with AstraLux, in both cases the detection is rather tentative, but since it is detected twice with consistent properties we count it as a genuine

detection. However, due to the poor quality of the fit and the fact that the two epochs of observation are only separated by three months, we do not try to acquire two epochs of astrometry, but merely quote the astrometry as the mean (and standard deviation) of the two epochs.

J04143060+2851298. J04143060+2851298 and J04143109+2851518, both from the Riaz et al. (2006) sample, are separated by only 23″ and although the estimated spectroscopic distances of 55 and 72 pc are not fully equal, they are consistent to within the 37% error. In addition, they have very similar proper motions (e.g., Röser et al. 2010) and thus probably form a physical pair.

J04244260−0647313. Although this star appears single in our images, it has been identified as a three-component spectroscopic multiple system in Shkolnik et al. (2010). The largest semimajor axis in the system is constrained as <0.25 AU, which at a distance of 35 pc corresponds to approximately <7 mas, hence we should indeed not expect to see any of these components in the AstraLux images.

J04305203−0849193. A known component of the wide binary Konigstuhl 2AB with a separation of 20″ (Caballero 2007), J04305203−0849193 is single closer in, in the AstraLux images.

J04373746−0229282. Better known as GJ 3305, this binary is part of the β Pic moving group (Zuckerman et al. 2001) and is also bound to 51 Eri in a wide orbit (Feigelson et al. 2006) with a projected separation of 66″. The binarity of GJ 3305 was first reported by Kasper et al. (2007) and has been observed with AstraLux on several occasions.

J04374563−0119118. The X-ray flux of this star is probably due to the fact that it is a symbiotic star, as identified by, e.g., Belczynski et al. (2000), hence we consider it as a contaminant to the Riaz et al. (2006) sample.

J04465175−1116476. J04465175−1116476 has a companion that has not yet been tested for common proper motion. Since the brightness and color match expectations, the system counts as an unconfirmed binary.

J05100427−2340407. Both J05100427−2340407 and J05100488−2340148 are binaries in the AstraLux images, so since they are separated by only 27″ on the sky and have very similar proper motions (e.g., Röser et al. 2010), this is likely a quadruple system in reality. Common proper motion remains to be confirmed for both of the close components.

J05130132−7027418. There is a companion to J05130132−7027418 in the AstraLux images which has a brightness and color that is consistent with a physical companion. It counts as an unconfirmed binary here, since it has not yet been tested for common proper motion.

J05195412−0723359. J05195412−0723359 and J05195513−0723399, both from the Riaz et al. (2006) sample, are separated by only 16″ and have comparable estimated distances (59 and 70 pc), as well as quite similar proper motions (e.g., Röser et al. 2010), and thus likely form a physical pair.

J05225705−0850119. This star has been classified as a probable T Tau star in Alcala et al. (1996).

J05243648−0535175. There is a possible companion at 7.″8 noted in WDS (Mason et al. 2001), but inside the AstraLux field of view, the star appears single.

J05301858−5358483. The AstraLux images resolve this system into a likely triple, where all components have brightnesses and colors consistent with a physically bound system. Since it has only been observed in one epoch, common proper motion has not yet been established.

J05320450−0305291. J05320450−0305291 is identified as a β Pic member in da Silva et al. (2009). It is also known as V1311 Ori.

J05323611−0523010. Also known as HR Ori, this star has been classified as a probable T Tau star in Alcala et al. (1996).

J05343767−0543044. J05343767−0543044 has been classified as a likely member of the ∼1 Myr Orion OBIc/d association (Stassun et al. 1999). The companion that was detected with AstraLux has not yet been confirmed to share a common proper motion, but its brightness and color are consistent with what would be expected for a physical companion, hence it is counted as such in the statistical analysis.

J05344858−3239362. All components of this triple system have colors and brightnesses consistent with expectation for physical companions. Common proper motion has however not yet been demonstrated.

J05350429−0508125. This star has been classified as a probable T Tau star in Alcala et al. (1996). It is also known as V1321 Ori.

J05355975−0616065. Also known as V1178 Ori, this star has been classified as a probable T Tau star in Alcala et al. (1996). It has a companion that is as of yet unconfirmed with regards to common proper motion, but since the brightness and color are well consistent with expectations for a real companion, the system is counted as binary in the statistics.

J06002304−4401217. The two components resolved by AstraLux have nearly equal brightnesses and colors. Hence, this counts as an unconfirmed binary, since the system has only been observed in one epoch so far.

J06061742−2754050. This star is likely a binary companion to the nearby K1-type star HD 41842 at 20″ separation, as noted in WDS (Mason et al. 2001).

J06112997−7213388. Since the separation between the components of this system is very small (∼0.″16), it is almost certainly a physical binary, although common proper motion has yet to be demonstrated.

J06134171−2815173. This binary consists of two components with almost equal brightnesses and colors. Although common proper motion has not yet been demonstrated, it thus counts as binary in the statistical analysis.

J06134539−2352077. The close binary pair which was resolved by AstraLux is likely itself a wide companion to the nearby G5-type star HD 43162 at 25″ separation, as noted in WDS (Mason et al. 2001). Hence, the system is likely triple, although common proper motion has not yet been demonstrated.

J06161032−1320422. In Bergfors et al. (2010), we detected a close binary companion to J06161032−1320422 at 190 mas separation. In a re-observation of the target from 2010 February, there is no resolved companion detected but only a slightly extended primary PSF, hence the binary separation probably decreased in the meantime.

J06234024−7504327. Although not yet confirmed to share a common proper motion, the companion to J06234024−7504327 is both relatively close ∼0.″57 and has consistent brightness and color to what should be expected for a physical companion.

J06262932−0739540. The motion in the J06262932−0739540 system is not yet sufficient to determine whether the two components share a common proper motion, but since the separation is small (∼0.″47) and the colors and brightnesses of the components are consistent with expectation, it is likely that they form a physical pair. The system counts as binary in the statistical analysis.

J06281861−0110504. The companion that was detected in the AstraLux images has not yet been confirmed as a physical companion through common proper motion. However, the two components have nearly equal brightness and colors, and a relatively small separation of ∼1.″4, hence it is very likely that it is a real physical binary, and it is counted as such here for statistical purposes.

J06351837+4745366. J06351837+4745366 is an unconfirmed binary with regards to common proper motion. Since the brightness and color of the companion is consistent with expectation, we count it as binary in the statistical analysis.

J06583980−2021526. Out of the targets that have been classified as "undetermined" with respect to common proper motion, the J06583980−2021526AB pair is one out of two that have reasonable (or even large) chances of being chance alignments rather than physical pairs. The fainter candidates J06583980−2021526C and D at larger separations reported in Bergfors et al. (2010) are clearly identified as background contaminants here, given both the colors and proper motions. However, J06583980−2021526B gives conflicting information. On one hand, its brightness and color are fully consistent with it being an almost equal-mass companion to the primary, which would be a very unusual coincidence for a background object, especially at a separation of only 1.″4. On the other hand, from an astrometric viewpoint, the B component is fully consistent with the expectation for a background object. The deviation from the background expectation is 0.4σ, and the B component has moved to a position that is 7.4 times closer to the background expectation than its first-epoch position, with a confidence for the motion of 7.5σ. This is also unlikely to happen by chance, hence the evidence is divergent. Since the magnitude of motion is not inconsistent with what could be expected for orbital motion of a real physical pair, we keep it as binary in our analysis, but we note that further observations will be necessary in order to resolve this issue satisfactorily.

J07115917−3510157. The two components of J07115917−3510157 have nearly equal brightnesses and colors, hence it is very likely that they form a physical pair. They have yet to be demonstrated to share a common proper motion.

J07210894+6739590. In addition to the close binarity discovered in the AstraLux data, there is a star at 21″ separation (HIP 35628), but due to its very different proper motion, it is likely physically unrelated to the J07210894+6739590 system (Reid et al. 2007).

J07282116+3345127. Although the star counts as single in our AstraLux data, it is in reality a spectroscopic binary with less than 0.55 AU semimajor axis, as noted by Shkolnik et al. (2010).

J07382951+2400088. A 2.″4 possible companion to J07382951+2400088 is noted in WDS (Mason et al. 2001), but our AstraLux images show no such companion.

J07505369+4428181. There is a companion to J07505369+4428181 which has a color and brightness that is consistent with what should be expected if it was physically bound. Common proper motion has not yet been tested for the system.

J08082487+4347557. Although the star counts as single in our AstraLux data, it is in reality a spectroscopic binary with less than 0.02 AU semimajor axis, as noted by Shkolnik et al. (2010).

J08224744−5726530. As noted in Bergfors et al. (2010), this is a triple system with component C outside of 6″. Hence, we do not include component C in Table 4, but we note that at 8.″429 ± 0.″001 separation in 2008.88 and 8.″374 ± 0.″003 in 2010.09, there is statistically significant orbital motion also for this component.

J08310177+4012115. For astrometric analysis of J08310177+4012115, we compare our AstraLux measurement with the data from the original discovery as listed in WDS (Mason et al. 2001). Since there are no error bars quoted, it is difficult to formally establish physical companionship. However, even if we assume that the errors are ±0.″5 and ±5°, which should be very conservative, the background hypothesis can still be firmly excluded with $\sim 5\sigma$ confidence. We therefore count it as a confirmed companion.

J08412528−5736021. The two components of this system have nearly equal colors and brightnesses, hence they very likely form a physical pair, although they have not yet been tested for common proper motion.

J08472279−4047381. This star is a known eclipsing binary with a period of 1.6219 days (Parihar et al. 2009), but has no additional companions in the AstraLux field of view.

J08475676−7854532. More commonly known as EQ Cha, this star appears single in the AstraLux images, but has most likely been partially resolved as a close binary in previous imaging campaigns (Köhler & Petr-Gotzens 2002; Brandeker et al. 2006). With an angular separation as small as 40 mas in 2003, it is fully plausible that the companion exists but was too close to be resolved by AstraLux in 2010.

J08483696−1353087. J08483696−1353087 and J08483645−1353083 are separated by only 7″, the former is a close binary (as of yet unconfirmed by common proper motion) and the latter is single, so this is likely a triple system in reality.

J09053033−4918382. This star has a probably brown dwarf companion, but since only one epoch of data exists, this is still unconfirmed.

J09121259−2555025. J09121259−2555025 has the alternative identifier CD-25 6962B in SIMBAD, implicitly implying companionship with the G2-type star CD-25 6962 at 14″ separation. However, given the apparently very different proper motions of the components (e.g., Röser et al. 2010), we consider such a companionship questionable.

J09164398−2447428. We resolve this star into a close binary (as of yet unconfirmed through common proper motion). It was recently classified as a classical Cepheid based on light curve analysis (Christiansen et al. 2008). We assume that this is a misclassification, given that the unresolved spectral type is M0.5V.

J09180165−5452332. J09180165−5452332 has a close (∼0.″49) companion to which it is probably physically bound, although this still needs to be confirmed through common proper motion.

J09365782−2610111. The companion discovered with AstraLux is probably physical given the rather small separation (∼0.″39), but so far only one epoch of imaging exists.

J09394631−4104029. This star is listed as a Tycho double star in the WDS catalog (Mason et al. 2000) with a separation of 600 mas and equal brightness. However, it appears entirely single in our AstraLux data. Although we cannot strictly rule out that the companion is presently too close to be resolved with AstraLux (e.g., due to a close to edge-on orbit and unfortunate timing of the observation), we consider it relevant to regard the possible companion as unconfirmed at present.

J09423823−6229028. The two components of this binary have almost equal brightnesses and colors, hence they are very likely to form a physical pair. Common proper motion has not yet been tested.

J10023100−2814280. J10023100−2814280 has a relatively close (∼0.″56) companion which is probably real, although this has yet to be confirmed with a proper-motion test.

J09583428−4625300. While the system appears single in the AstraLux images, it is in reality a spectroscopic binary with a 1.88 day period (e.g., Diáz et al. 2007). Such a small orbit is obviously consistent with a non-detection by AstraLux.

J10162867−0520320. In this previously known system, J10162867−0520320 is a spectroscopic binary of two M-dwarfs components, which is in turn a visual companion at 3.″2 separation from a WD. Furthermore, the WD is itself a spectral binary, making the system quadruple, with a demonstrated physical companionship of all four components (Vennes et al. 1999). The 3.″2 pairing is easily distinguished in the AstraLux image, but the spectroscopic pairs remain unresolved. Because the system must primordially have had a pre-WD primary much more massive than J10162867−0520320 (given that the main-sequence lifetime of an M0 star is longer than the Hubble time), we do not count it as an M-star binary for any of our statistical purposes. The binary is listed as having confirmed proper motion in Table 4, this is based on the result in Vennes et al. (1999) and not our comparison with the astrometric point in the literature; since no error bars are listed for that point and since we only get rather marginally significant results if we assume reasonable errors of 0.″1 and 1°, we do not draw any new conclusions on the basis of such a comparison.

J10181387−2028413. The star is single in the AstraLux images, but has a known wide companion at 32″ separation (Deacon & Hambly 2007).

J10423011−3340162. The source at 2.″4 separation, first reported in Neuhäuser et al. (2000), is an already known background star (Lowrance et al. 2005), a conclusion which we can confirm at ∼28σ confidence.

J11091380−3001398. This previously known binary (e.g., Webb et al. 1999) is part of the TW Hya association and is also known as TWA 2.

J11102788−3731520. This previously known binary (e.g., Brandeker et al. 2003) is part of the TW Hya association and is also known as TWA 3.

J11240434+3808108. There is a possible brown dwarf companion to J11240434+3808108 at 8″ separation noted by Reid et al. (2007), but it is single within the AstraLux field of view.

J11254754−4410267. J11254754−4410267 has a relatively close (∼0.″55) companion that is likely physically bound, but so far there is only a single epoch of data available.

J11315526−3436272. This system has been identified as a member of the TW Hya association (Kastner et al. 1997) and is known as TWA 5. It contains a previously known brown dwarf TWA 5B, first suggested by Lowrance et al. (1999) and later confirmed by, e.g., Brandeker et al. (2003). The latter also reported the presence of a close companion TWA 5Ab at 54 mas from the primary, independently detected by Macintosh et al. (2001). We detect TWA 5B in our AstraLux data, but not TWA 5Ab, which implies that the projected separation was probably smaller in 2010 than it was in 2000. The orbit of TWA 5Aa/Ab has been analyzed in detail by Konopacky et al. (2007). Using the orbital parameters that they determine, we deduce that at epoch 2010.11, the projected separation should be only about 18 mas, which is well consistent with our non-detection of TWA 5Ab. We use the best-fit total mass of 0.71 $M_{\odot}$ for TWA 5Aa/Ab from Konopacky et al. (2007).

J12045611+1728119. Common proper motion is shared between J12045611+1728119 and HIP 58919 at 23″ separation, hence they constitute a wide physical pair (Lépine & Bongiorno 2007).

J12062214−1314559. Due to the small separation (∼0.″42) of the companion detected in the AstraLux images, it is likely a physical companion, although common proper motion has not yet been tested.

J1206557+700749. Aside from the spatially resolved companion, the primary in the J1206557+700749 system is a known spectroscopic binary with a semimajor axis less than 0.03 AU. This is well consistent with our AstraLux data, where the primary is significantly brighter than the secondary, despite having about equal spectral type. Hence, the system is a triple in reality.

J12134173−1122405. A companion to J12134173−1122405 is detected in the AstraLux images which has not yet been tested for common proper motion, but the color and brightness is consistent with the expectation for a physically bound companion.

J12173945−6409418. The two targets J12173945−6409418 and J12174012−6409389 are physically bound, as shown by common proper-motion analysis. However, this means that one of the targets likely has an error in the Riaz et al. (2006) spectral-type determination, since J12174012−6409389 is classified as M2 but is fainter than J12174012−6409389, which is classified as M3.5. The fact that J12174012−6409389 is fainter holds true both in 2MASS and in the AstraLux images. Both components are resolved as close binaries with AstraLux, so we consider it a strong candidate for a quadruple system, with J12173945−6409418A as the primary. Concerning which spectral-type determination is incorrect, we consider that it is more likely that J12174012−6409389 is misclassified, as the flux ratio to the close companion is closer to unity than in the J12174012−6409389 case. We thus set the spectral type of J12174012−6409389A to M3 ± 1, and determine the other spectral types on the basis of flux ratios. Component Bb is not visible in the i' data, but becomes visible in z' thanks to the higher Strehl ratio and intrinsic brightness of the component. A fifth object is visible in the field, but its color reveals it to be a likely background star.

J12345629−4538075. J12345629−4538075 is better known as TWA 16. The presence of a close companion to this star was noted in Zuckerman et al. (2001) which seems to be consistent with the companion that we detect. However, since no explicit astrometric information is given in Zuckerman et al. (2001) other than a rough estimation of the separation (0.″67), it is not possible to test whether the companion shares a common proper motion with the primary at this point. The brightness and color are consistent with a physical companion, hence the system counts as binary in the statistics.

J12351726+1318054. The position angle for this system given in Law et al. (2006) is actually 257.°0, but since the components are fairly similar in brightness and there is a fake triplet effect, we assume that there can be a 180° phase shift present in the Law et al. (2006) data (or alternatively in both of our epochs). The angular motion in our two AstraLux images is 1.°8 in about 0.5 years. If taken at face value, then the Law et al. (2006) data point would imply 198.°4 angular motion in 4.5 years, corresponding to 22° per half-year, which is an order of magnitude too large. On the other hand, if we subtract 180° from the Law et al. (2006) position angle to get 77.°0, then the angular motion is 2.°0 per half-year, which is perfectly consistent

with our measurements. Hence, we adopt the latter value for our analysis.

J12392104−5337579. The two components of J12392104−5337579 that were detected in the AstraLux images have almost equal brightnesses and color, hence they are very likely physically bound. Common proper motion has not yet been tested.

J12485345+1204326. J12485345+1204326 is a wide (76″) common proper-motion companion to HIP 62536 (Lépine & Bongiorno 2007), but is single in the AstraLux images.

J12533626+2247354. The star shows photometric variability with a 1.9 day periodicity (Norton et al. 2007).

J12565215+2329501. J12565215+2329501 and J12565272+2329506 constitute a known 8″ binary pair in the Reid et al. (2007) sample.

J13013268+6337496. Aside from the binary companion detected in the AstraLux images, the star has a probable wide companion at 119″, as noted in WDS (Mason et al. 2001).

J13015919+4241160. The companion to the J13015919+4241160 is clearly inconsistent with a background contaminant, but the astrometry is also inconsistent with a simple orbital motion of B around A—for instance, the separation decreases from 2008 June to 2009 February, but then increases again to 2009 June. This could, for instance, imply that either A or B is a close unresolved binary, where the photocenter shifts on a shorter timescale than that of the AB orbit.

J13022691−5200507. Due to the very compact arrangement of the three components of J13022691−5200507, it is highly probable that this is a physically bound triple system. Furthermore, the system is conspicuously close to the close binary J13025257−5201384 both on the sky and in distance (52 versus 59 pc), hence this is a candidate quintuple system. Only one epoch of imaging exists, so common proper motion has not yet been demonstrated.

J13082484+3019094. Aside from the binary companion detected in the AstraLux images, the star has a possible wide companion at 101″, as noted in WDS (Mason et al. 2001).

J13093495+2859065. Also known as GJ 1167 A, this star has a wide companion at about 190″ according to WDS (Mason et al. 2001).

J13120689+3213179. J13120525+3213332 and J13120689+3213179 constitute a known 26″ binary pair in the Reid et al. (2007) sample, and in addition, each of the components are discovered as close binaries in the AstraLux data. Hence, the system is a very likely quadruple system, although the close pair of J13120689+3213179 has yet to be formally confirmed as physically bound.

J13151846−0249516. Due to the small separation of the companion to J13151846−0249516, it is very likely a physical binary, but common proper motion has not yet been tested for.

J13195689−6831142. J13195689−6831142 has a companion detected in the AstraLux images. Since the companion is relatively close (∼0.″88) and has a brightness and color that is consistent with expectation, it is probably a physical pair. Only one epoch of images exists so far.

J13293209+5142114. The B component seen in the AstraLux images appears to be a very close binary itself due to a PSF extension visible in five separate epochs. However, we count the system as a regular binary here since we do not get a converging fit for the closer pair.

J13313493+5857171. We count J13313493+5857171 as single close in, although its PSF appears somewhat extended in the 2009.13 epoch. However, it is a likely companion to the nearby G2-star HD 117845 at 11″ separation. HD 117845 has been included in the AstraLux field and appears to be itself a close binary with a ∼0.″5 separation.

J13345147+3746195. Although the close binarity of J13345147+3746195 was reported in Daemgen et al. (2007) and our AstraLux data have a similar sensitivity, the star appears single in our images. Since the separation was only 82 mas in 2006, it has presumably moved inward since then.

J13493313−6818291. Due to the compact configuration of the three components resolved by AstraLux, the probability is very high for this to constitute a physical triple system. Common proper motion has not yet been tested for.

J13534589+5210298. The secondary detected in the AstraLux images is perhaps itself a close binary, as it appears extended in epochs 2008.64 and 2009.42. However, we count it as a single component of the system here.

J14134677+4618227. J14134677+4618227 is possibly a wide companion to HIP 69518 at 83″ (Reid et al. 2007). It is however single in the AstraLux field of view.

J14201961+2758563. This star is variable and has been classified as a classical Cepheid based on this variability (Akerlof et al. 2000). We assume that this is a misclassification, given that the spectral type is K5.

J14204953+6049348. Although the star is single in our AstraLux images, it is known to be a spectroscopic binary with a semimajor axis of 0.01 AU (Shkolnik et al. 2010).

J14402293+1339230. This late-type (M7.5–M8.0) object is classified as a brown dwarf in SIMBAD. It is however unclear what this classification is based on, as our comprehensive search through the full published body of literature available on the object did not turn up any references or justification to such a classification.

J14433804−0414354. The two components resolved by AstraLux have very similar brightnesses and colors, hence physical companionship is probable, although common proper motion has not yet been tested for.

J15090696+5904282. J15090696+5904282 and J15090808+5904258 are separated by only 9″ and have similar estimated spectroscopic distances (30 and 39 pc, respectively) in Riaz et al. (2006), hence it is likely that they form a physical pair.

J15235385+5609320. A probable wide companion to this star at approximately 68″ separation is noted in WDS (Mason et al. 2001).

J15370409+3748275. The star displays photometric variability at a 1.2 day period (Norton et al. 2007).

J15530484+4457446. The close binary that we discovered in the AstraLux images was not seen in the Daemgen et al. (2007) study with a similar spatial resolution, which implies that the projected separation of the system probably increased during the intermediate period.

J15553178+3512028. In addition to the astrometric points listed in Table 4, there is another data point from 2005 in Law et al. (2008). This point is essentially at equal epoch to the Daemgen et al. (2007) point, but the position angle differs by 88° in the two cases. While the Daemgen et al. (2007) data point is fully consistent with all other astrometric points of the target, the Law et al. (2008) point is fully inconsistent in this regard. The close to 90° offset could imply some trivial trigonometric error in Law et al. (2008). Here, we simply exclude the point from our analysis.

J16291031+7804399. Like J10162867-0520320, this is a previously known system with a WD component (Farihi et al.

2010). Hence, we do not include this system in the binary fraction statistics.

J16494292+2220037. The star shows photometric variability with a 22.9 day periodicity, which might imply that it is an eclipsing binary (Norton et al. 2007).

J16552880−0820103. Also known as GJ 644, this is a well known and much studied triple system (e.g., Ségransan et al. 2000), of which we resolve the wider AB pair (the secondary is a spectroscopic binary with a 3 day period). In addition, there are two much wider components known to share a common proper motion with GJ 644, making the system a likely quintuple. Since there are so many existing astrometric points of the AB pair in the literature, we do not give an extensive list in Table 4, but rather refer the reader to Ségransan et al. (2000), where there is a full orbital analysis of the close triple system.

J16590962+2058160. The star displays photometric variability at a 4.1 day period (Norton et al. 2007).

J17111769+1245408. J17111769+1245408 and J17111841+1245080, both from the Riaz et al. (2006) sample, are separated by only 34″ and have comparable estimated distances (69 and 82 pc), as well as similar proper motions (e.g., Röser et al. 2010), and thus likely form a physical pair.

J17292722+3524048. This star is variable and has been classified as a classical Cepheid based on this variability (Akerlof et al. 2000). We assume that this is a misclassification, given that the spectral type is K5.

J17380077+3329457. The B component of the system appears to be a close binary itself in several different epochs of AstraLux imaging, but the suspected Ba/Bb pair is not sufficiently resolved to get a converging binary fit, hence we treat the AB system as a regular binary in this study.

J18153459+1614253. A possible wide companion to J18153459+1614253 at 13″ is noted in WDS (Mason et al. 2001). The star is however single within the AstraLux field of view.

J18351833+4544379. Also known as GJ 720 A, this star has a wide companion with a demonstrated common proper motion at about 112″ according to Lépine & Bongiorno (2007).

J18355276+1659057. J18355276+1659057 is possibly a wide companion to HIP 91159 at 35″ separation, as noted in Reid et al. (2007).

J18464053−0916238. The primary star has two candidate companions in the field of view. The fainter candidate C is most likely a background star, since its color is entirely inconsistent with a late M-type star. The brighter candidate B is more uncertain. Its colors are fully consistent with the brightness contrast to the primary for a physical companion, implying a spectral type of M5. It is also visible in 2MASS (Skrutskie et al. 2006), which enables us to perform a rough common proper motion (CPM) test. The test indicates that B is inconsistent with a static background object, again implying physical companionship. However, the motion is also poorly consistent with orbital motion, with a sky-projected speed of order 2 AU per year—highly unlikely for such a wide and low-mass binary. This implies either underestimated uncertainties in the data, or an unusual astronomical coincidence. With the small separation and relatively high brightness difference of the candidate companion, it is just at the detection limit of 2MASS and is only reliably detectable in K band. Perhaps there is a systematic noise component beyond the quoted astrometric 2MASS error in this circumstance. If all the data are taken at face value, then another possible interpretation is an unfortunate chance alignment with a local M-dwarf, which has a significant proper motion of its own. In any case, due to all these uncertainties, we tentatively treat the pair as a candidate binary here, but emphasize that more data are needed to test physical companionship.

J18564143+5014071. J18564143+5014071 and J18564286+5013483 are separated by only 23″ and have similar estimated spectroscopic distances (79 and 77 pc, respectively) in Riaz et al. (2006), as well as very similar proper motions (e.g., Röser et al. 2010), hence it is likely that they form a physical pair.

J19105480+3017476. The AstraLux images reveal three components in the J19105480+3017476 system. Due to their very compact configuration, the triple system is very likely physically bound. Only one epoch of imaging exists so far.

J19213210+4230520. The very close companion resolved by AstraLux is probably physically bound, but this has yet to be tested through proper-motion analysis.

J19425324−4406278. A close companion to J19425324−4406278 is detected which is counted as a physical companion for statistical purposes, although this has not yet been demonstrated through common proper motion.

J19432464−3722108. Only one epoch of imaging exists for this binary system, hence common proper motion has not yet been confirmed. It is counted as an unconfirmed binary here.

J20003177+5921289. Aside from the close companion detected in the AstraLux data, J20003177+5921289 possibly has a wide companion at 14″, as noted in WDS (Mason et al. 2001).

J20100002−2801410. Given the relatively small separation (∼0.″62) and the similar brightnesses of the two components in the J20100002−2801410 system, it is likely that they form a physical pair. However, only one epoch of imaging exists at this point.

J20163382−0711456. Due to the very small separation of the detected companion to J20163382−0711456, this is likely to be a physical binary, although a second epoch to confirm common proper motion has not yet been acquired.

J20500010−1154092. J20500010−1154092 has a close companion detected with AstraLux, but it has not yet been confirmed through common proper motion. However, since the separation is quite small (∼0.″47) and the brightness and color of the companion is consistent with expectations, the system counts as binary for statistical purposes.

J20564846−0450490. This star has a wide companion at about 14″ as noted in, e.g., the WDS catalog (Mason et al. 2001). It is however single in the separation range covered by the AstraLux data.

J20581756+1541315. J20581756+1541315 and J20581836+1541211, both from the Riaz et al. (2006) sample, are separated by only 10″ and have comparable estimated distances (144 and 119 pc), as well as similar proper motions (e.g., Röser et al. 2010) and thus likely form a physical pair.

J21091375−0814041. The binary J21091375−0814041 is as of yet unconfirmed with regards to common proper motion, but the components have similar colors and brightnesses, and a relatively small separation of ∼0.″97, hence the pair is probably physically bound and counts as such in the statistical analysis.

J21154192+1746242. This star possibly has a wide companion at about 9″ as noted in, e.g., the WDS catalog (Mason et al. 2001). It is however single in the separation range covered by the AstraLux data.

J21205172−0301545. J21205172−0301545 has a companion with brightness and color that is consistent with expectation, but no common proper motion test has yet been done.

Table 5
Properties of Probable Background Stars

2MASS ID	$\Delta z'$ (mag)	$\Delta i'$ (mag)	ρ ($''$)	θ ($^{\circ}$)	Epoch	Comment
J01365516−0647379AB	5.45 ± 0.01	5.11 ± 0.01	5.580 ± 0.007	180.6 ± 0.3	2008.63	Off color
J04133532+1541016AB	−0.85 ± 0.43	−1.26 ± 0.27	5.609 ± 0.003	289.1 ± 0.3	2008.63	Non-CPM
J06141327−0035516AB	5.49 ± 0.29	5.18 ± 0.21	5.749 ± 0.002	320.1 ± 0.3	2008.02	Off color
J06315741−0832494AB	2.51 ± 0.01	2.52 ± 0.01	5.628 ± 0.003	107.7 ± 0.3	2008.02	Off color
J06583980−2021526AD	6.91 ± 0.03	...	5.149 ± 0.001	253.9 ± 0.3	2008.87	Unclear case
J07174710−2558554AB	6.35 ± 0.04	...	5.332 ± 0.002	126.8 ± 0.3	2008.88	Unclear case
J07184418−2616172AB	8.27 ± 0.11	8.63 ± 0.14	2.733 ± 0.015	247.4 ± 0.3	2010.08	Unclear case
J08471906−5717547AB	6.78 ± 0.09	7.63 ± 0.14	5.724 ± 0.014	326.6 ± 0.3	2010.09	Unclear case
J09180165−5452332AC	3.48 ± 0.04	2.80 ± 0.02	2.880 ± 0.011	259.5 ± 0.3	2010.08	Off color
J09345604−7804193AC	4.37 ± 0.08	4.05 ± 0.07	1.959 ± 0.014	227.3 ± 0.3	2010.10	Off color
J10000855−5401196AB	7.53 ± 0.10	7.09 ± 0.11	3.055 ± 0.015	250.3 ± 0.3	2010.08	Off color
J10423011−3340162AB	8.42 ± 0.10	8.02 ± 0.20	3.279 ± 0.014	119.3 ± 0.3	2010.08	Non-CPM
J11134086−6448593AB	7.31 ± 0.09	6.53 ± 0.10	1.795 ± 0.014	280.4 ± 0.3	2010.08	Off color
J11134086−6448593AC	6.25 ± 0.09	6.52 ± 0.11	5.288 ± 0.014	0.9 ± 0.3	2010.08	Off color
J12392104−5337579AC	5.67 ± 0.10	5.15 ± 0.09	5.080 ± 0.014	237.0 ± 0.3	2010.10	Off color
J12392104−5337579AD	5.96 ± 0.10	5.97 ± 0.11	4.530 ± 0.015	268.0 ± 0.3	2010.10	Off color
J12405202−6856585AB	7.16 ± 0.09	7.46 ± 0.11	2.694 ± 0.014	292.1 ± 0.3	2010.10	Unclear case
J13493313−6818291AD	3.24 ± 0.05	3.19 ± 0.02	4.562 ± 0.011	70.5 ± 0.3	2010.10	Off color
J14190331+6451463AB	4.97 ± 0.01	4.89 ± 0.01	4.653 ± 0.005	34.7 ± 0.3	2008.45	Non-CPM
J14450627+4409393AB	4.36 ± 0.17	3.70 ± 0.17	5.233 ± 0.004	114.3 ± 0.3	2008.64	Non-CPM
J14511044+3106406AB	5.50 ± 0.86	5.42 ± 0.82	2.353 ± 0.005	48.3 ± 0.3	2008.45	Off color
J16460779+4142057AB	4.27 ± 0.07	3.82 ± 0.04	5.672 ± 0.001	336.7 ± 0.3	2009.42	Non-CPM
J16503028+2319353AB	0.54 ± 0.05	0.47 ± 0.05	2.373 ± 0.001	114.1 ± 0.3	2008.45	Off color
J17261439+1404364AB	7.84 ± 0.60	6.58 ± 0.60	2.029 ± 0.025	248.6 ± 1.0	2008.45	Off color
J17261439+1404364AC	8.92 ± 0.48	8.02 ± 0.48	5.007 ± 0.002	93.2 ± 0.3	2008.45	Off color
J18064367+6822031AB	5.57 ± 0.53	5.10 ± 0.31	5.301 ± 0.002	124.4 ± 0.3	2008.45	Off color
J18464053−0916238AC	5.82 ± 0.03	5.87 ± 0.04	5.777 ± 0.011	204.6 ± 0.3	2008.45	Off color
J18471129+2212413AC	4.18 ± 0.32	4.05 ± 0.12	4.795 ± 0.007	29.3 ± 0.3	2009.42	Off color
J21150531−0949414AB	4.17 ± 0.04	4.17 ± 0.04	3.793 ± 0.006	233.4 ± 0.3	2008.88	Off color
J22413577+2602128AB	7.22 ± 0.62	6.69 ± 0.34	3.533 ± 0.036	65.9 ± 0.5	2007.84	Off color

J21295166−0220070. The close companion to J21295166−0220070 has consistent brightness and color with the expectation for a physical companion. Only one epoch of images exists, hence common proper motion has yet to be confirmed.

J21365560−0840313. Due to the small separation (∼0.″24) of the companion detected in the AstraLux images, physical companionship is very likely, although only one epoch of images exists so far.

J22014336−0925139. The two components of the J22014336−0925139 system that have been resolved with AstraLux have very similar brightnesses and colors, and it is therefore likely that they form a physical binary pair. Common proper motion has not yet been demonstrated.

J22171899−0848122. This system counts as a single in our statistics, even though it appears to be a triple system in reality. The reason for this is that the A component was the AstraLux target, and the BC pair at ∼7.″8 is outside of the completeness cutoff at 6″. Since the BC pair is visible in the AstraLux images, we can nonetheless analyze it astrometrically. This pair was first reported by Beuzit et al. (2004) with $\rho = 0.''978$ and $\theta = 305.^{\circ}8$. There are no error bars quoted, but if we assume that the quoted precision in decimal places corresponds to the measurement precision, and adopt errors of 5 mas and 0.°5, which should be conservative in that circumstance, we find that common proper motion can be confirmed at a 76σ confidence level. Hence, physical companionship can be confidently inferred, even if the errors should be substantially larger than what we have assumed.

J22232904+3227334. Also known as GJ 856, this is a well-studied binary with several astrometric data points over a long baseline. In Table 4, we present the AstraLux data as well as one example data point from the literature, and otherwise refer to Seymour et al. (2002) for more information on the astrometric data and a preliminary orbit fit. López-Santiago et al. (2006) classify the system as a member of subgroup B4, with an estimated age of ∼100 Myr.

J22545501+2414451. This star has a probable wide companion at about 73″ as noted in, e.g., the WDS catalog (Mason et al. 2001). It is however single in the separation range covered by the AstraLux data.

J23062378+1236269. In addition to the previously known binary companion seen in the AstraLux images, J23062378+1236269 is also a spectroscopic binary with a semimajor axis smaller than 0.31 AU (Shkolnik et al. 2010) and has the additional wide companion J23062530+1236570 (also in the sample, a single star in the AstraLux images) at 37.″6 with confirmed proper motion (Lépine & Bongiorno 2007), hence the system is likely quadruple in reality.

J23062928−0502285. The M7.5 spectral-type classification of J23062928−0502285 originates from a spectroscopic analysis in Gizis et al. (2000). There is some ambiguity to this classification in that Bouy et al. (2003) find it to be a brown dwarf of type L4. However, the latter estimate is based on a single color, so we consider it less reliable.

J23101857+1447203. The star is classified as T Tau in Li et al. (2000).

J23120603+2655579. As noted in Lépine & Bongiorno (2007), J23120603+2655579 forms a probable wide (14″) pair with HIP 114543, which is itself a 1″ binary. Hence, with the additional component seen in the AstraLux images, the system is likely quadruple.

J23205766−0147373. Although the close binarity of J23205766−0147373 was reported in Daemgen et al. (2007) and our AstraLux data have a similar sensitivity, the star appears single in our images. Since the separation was only 99 mas in 2005, it has presumably moved inward since then.

J23230117−0635436. There is a spectral classification ambiguity for this target, with a K5 classification in Riaz et al. (2006) and a G9III classification in SIMBAD. Regardless of which one is trusted, the star is too early-type to be included in the statistical studies anyway.

J23261707+2752034. A very close (∼0.″15) companion is detected, which is most likely physically bound, although this has yet to be confirmed with common proper motion.

J23314492−0244395. There is a possible companion at 19″ noted in Lowrance et al. (2005), but it has not been checked for common proper motion.

J23342274+2739556. This star has a possible wide companion at about 63″ as noted in, e.g., the WDS catalog (Mason et al. 2001). It is however single in the separation range covered by the AstraLux data.

J23385413−1246184. This late-type (M6.5) object is classified as a brown dwarf in SIMBAD. It is however unclear what this classification is based on, as our comprehensive search through the full published body of literature available on the object did not turn up any references or justification to such a classification.

J23450477+1458573. Due to the compact configuration of the three components resolved by AstraLux, this is almost certainly a physically bound triple system. Only one epoch of images exist so far, hence common proper motion has not yet been demonstrated.

APPENDIX B

BACKGROUND STARS

In Table 5, we summarize the objects detected in the AstraLux images that have been identified as probable (or in some cases near-certain) background objects.

REFERENCES

Akerlof, C., Amrose, S., Balsano, R., et al. 2000, AJ, 119, 1901
Alcala, J. M., Terranegra, L., Wichmann, R., et al. 1996, A&AS, 119, 7
Basu, S., & Vorobyov, E. I. 2012, ApJ, 750, 30
Bate, M. R. 2009, MNRAS, 392, 590
Bate, M. R. 2012, MNRAS, 419, 3115
Belczynski, K., Mikolajewska, J., Munari, U., Ivison, R. J., & Friedjung, M. 2000, A&AS, 146, 407
Bergfors, C., Brandner, W., Janson, M., et al. 2010, A&A, 520, 54
Beuzit, J.-L., Ségransan, D., Forveille, T., et al. 2004, A&A, 425, 997
Bourke, T. L., Myers, P. C., Evans, N. J., II., et al. 2006, ApJ, 649, L37
Bouy, H., Brandner, W., Martin, E., et al. 2003, AJ, 126, 1526
Bouy, H., Duchêne, G., Köhler, R., et al. 2004, A&A, 423, 341
Brandeker, A., Jayawardhana, R., Khavari, P., Haisch, K. E., & Mardones, D. 2006, ApJ, 652, 1572
Brandeker, A., Jayawardhana, R., & Najita, J. 2003, AJ, 126, 2009
Burgasser, A., Kirkpatrick, J. D., Reid, I. N., et al. 2003, ApJ, 586, 512
Burgasser, A., Reid, I. N., Siegler, N., et al. 2007, in Protostars and Planets V, ed. B. Reipurth, D. Jewitt, & K. Kiel (Tucson, AZ: Univ. Arizona Press), 427
Burrows, A., Marley, M., Hubbard, W.' B., et al. 1997, ApJ, 491, 856
Caballero, J. A. 2007, ApJ, 667, 520
Casewell, S. L., Jameson, R. F., & Burleigh, M. R. 2008, MNRAS, 390, 1517
Chabrier, G., Baraffe, I., Allard, F., & Hauschildt, P. 2000, ApJ, 542, 464
Chauvin, G., Lagrange, A.-M., Bonavita, M., et al. 2010, A&A, 509, 52
Chen, W. P., Sanchawala, K., & Chiu, M. C. 2006, AJ, 131, 990
Christiansen, J. L., Derekas, A., Kiss, L. L., et al. 2008, MNRAS, 385, 1749
Close, L. M., Siegler, N., Freed, M., & Biller, B. 2003, ApJ, 587, 407
Correia, S., Zinnecker, H., Ratzka, T., & Sterziki, M. F. 2006, A&A, 459, 909
Daemgen, S., Hormuth, F., Brandner, W., et al. 2009, A&A, 498, 567
Daemgen, S., Siegler, N., Reid, I. N., & Close, L. M. 2007, ApJ, 654, 558
da Silva, L., Torres, C. A. O., de La Reza, R., et al. 2009, A&A, 508, 833
Davis, P. J., Kolb, U., & Willems, B. 2010, MNRAS, 403, 179
Deacon, N. R., & Hambly, N. C. 2007, A&A, 468, 163
Delfosse, X., Beuzit, J.-L., Marchal, L., et al. 2004, in ASP Conf. Ser. 381, Spectroscopically and Spatially Resolving the Components of Close Binary Stars, ed. R. W. Hilditch, H. Hensberge, & K. Pavlovski (San Francisco, CA: ASP), 166
Delfosse, X., Forveille, T., Ségransan, D., et al. 2000, A&A, 364, 217
Delorme, P., Lagrange, A. M., Chauvin, G., et al. 2012, A&A, 539, 72
Díaz, R. F., González, J. F., Cincunegui, C., & Mauas, P. J. D. 2007, A&A, 474, 345
Dupuy, T. J., & Liu, M. C. 2011, ApJ, 733, 122
Duquennoy, A., & Mayor, M. 1991, A&A, 248, 485
Eisenhauer, F., Perrin, G., Brandner, W., et al. 2011, Messenger, 143, 16
Farihi, J., Becklin, E. E., & Zuckerman, B. 2005, ApJS, 161, 394
Farihi, J., Hoard, D. W., & Wachter, S. 2010, ApJS, 190, 275
Feigelson, E. D., Lawson, W. A., Stark, M., Townsley, L., & Garmire, G. P. 2006, AJ, 131, 1730
Fischer, D., & Marcy, G. 1992, ApJ, 396, 178
Gizis, J. E., Monet, D. G., Reid, I. N., et al. 2000, AJ, 120, 1085
Gizis, J. E., Reid, I. N., Knapp, G. R., et al. 2003, AJ, 125, 3302
Goodwin, S. P., Kroupa, P., Goodman, A., & Burkert, A. 2007, in Protostars and Planets V, ed. B. Reipurth, D. Jewitt, & K. Kiel (Tucson, AZ: Univ. Arizona Press), 133
Goodwin, S. P., & Whitworth, A. 2007, A&A, 466, 943
Gould, A., & Chanamé, J. 2004, ApJS, 150, 455
Harrington, R. S., & Dahn, C. C. 1980, AJ, 85, 454
Henry, T. J., Jao, W.-C., Subsavage, J. P., et al. 2006, AJ, 132, 2360
Hillenbrand, L. A., & White, R. J. 2004, ApJ, 604, 741
Hippler, S., Bergfors, C., Brandner, W., et al. 2009, Messenger, 137, 14
Hormuth, F., Brandner, W., Hippler, S., Janson, M., & Henning, T. 2007, A&A, 463, 707
Hormuth, F., Hippler, S., Brandner, W., Wagner, K., & Henning, T. 2008, Proc. SPIE, 7014, 138
Janson, M., Brandner, W., Lenzen, R., et al. 2007, A&A, 462, 615
Jao, W.-C., Henry, T. J., Subsavage, J. P., et al. 2003, AJ, 125, 332
Jenkins, L. F. 1952, General Catalog of Trigonometric Stellar Parallaxes (1st ed.; New Haven, CT: Yale Univ. Observatory)
Joergens, V. 2008, A&A, 492, 545
Kasper, M., Apai, D., Janson, M., & Brandner, W. 2007, A&A, 472, 321
Kastner, J. H., Zuckerman, B., Weintraub, D. A., & Forveille, T. 1997, Science, 277, 67
Köhler, R. 2001, AJ, 122, 3325
Köhler, R., & Petr-Gotzens, M. G. 2002, AJ, 124, 2899
Köhler, R., Ratzka, T., Herbst, T. M., & Kasper, M. 2008, A&A, 482, 929
Konopacky, Q. M., Ghez, A., Barman, T. S., et al. 2010, ApJ, 711, 1087
Konopacky, Q. M., Ghez, A., Duchene, G., McCabe, C., & Macintosh, B. A. 2007, AJ, 133, 2008
Kouwenhoven, M. B. N., Brown, A. G. A., Portegies Zwart, S. F., & Kaper, L. 2007, A&A, 474, 77
Kraus, A. L., & Hillenbrand, L. A. 2007, AJ, 134, 2340
Law, N. M. 2006, PhD thesis, Inst. Astronomy & Selwyn College, Cambridge Univ.
Law, N. M., Hodgkin, S. T., & Mackay, C. D. 2006, MNRAS, 368, 1917
Law, N. M., Hodgkin, S. T., & Mackay, C. D. 2008, MNRAS, 384, 150
Lépine, S., & Bongiorno, B. 2007, AJ, 133, 889
Lépine, S., & Gaidos, E. 2011, AJ, 142, 138
Lépine, S., Thorstensen, J. R., Shara, M. M., & Rich, R. M. 2009, AJ, 137, 4109
Li, J. Z., & Hu, J. Y. 1998, A&AS, 132, 173
Li, J. Z., Hu, J. Y., & Chen, W. P. 2000, A&A, 356, 157
Liu, M. C., Dupuy, T. J., & Ireland, M. J. 2008, ApJ, 689, 436
López-Santiago, J., Montes, D., Crespo-Chacón, I., & Fernández-Figueroa, M. J. 2006, ApJ, 643, 1160
Lowrance, P. J., Becklin, E. E., Schneider, G., et al. 2005, AJ, 130, 1845
Lowrance, P. J., McCarthy, C., Becklin, E. E., et al. 1999, ApJ, 512, L69
Luhman, K. L., Lada, C. J., Hartmann, L., et al. 2005, ApJ, 631, 69
Macintosh, B., Max, C., Zuckerman, B., et al. 2001, in ASP Conf. Ser. 244, Young Stars Near the Earth: Progress and Prospects, ed. R. Jayawardhana & T. P. Greene (San Fransisco, CA: ASP), 309

Mamajek, E. E. 2005, ApJ, 634, 1385
Mason, B. D., Hartkopf, W. I., Gies, D. R., Henry, T. J., & Helsel, J. W. 2009, AJ, 137, 3358
Mason, B. D., Wycoff, G. L., Hartkopf, W. I., Douglass, G. G., & Worley, C. E. 2001, AJ, 122, 3466
Mason, B. D., Wycoff, G. L., Urban, S. E., et al. 2000, AJ, 120, 3244
McCarthy, C., Zuckerman, B., & Becklin, E. E. 2001, AJ, 121, 3259
Morlet, G., Salaman, M., & Gili, R. 2002, A&A, 396, 933
Neuhäuser, R., Brandner, W., Eckart, A., et al. 2000, A&A, 354, 9
Norton, A. J., Wheatley, P. J., West, R. G., et al. 2007, A&A, 467, 785
Parihar, P., Messina, S., Bama, P., et al. 2009, MNRAS, 395, 593
Perryman, M. A. C., Lindegren, L., Kovalevsky, J., et al. 1997, A&A, 323, 49
Peter, D., Feldt, M., Henning, T., & Hormuth, F. 2012, A&A, 538, 74
Quirrenbach, A., Amado, P. J., Mandel, H., et al. 2010, Proc. SPIE, 7735, 37
Raghavan, D., McAlister, H. A., Henry, T. J., et al. 2010, ApJS, 190, 1
Reid, I. N., & Cruz, K. L. 2002, AJ, 123, 2806
Reid, I. N., Cruz, K. L., Allen, P., et al. 2004, AJ, 128, 463
Reid, I. N., Cruz, K. L., & Allen, P. R. 2007, AJ, 133, 2825
Reidel, A. R., Subasavage, J. P., Finch, C. T., et al. 2010, AJ, 140, 897
Reipurth, B., & Clarke, C. 2001, AJ, 122, 432
Riaz, B., Gizis, J., & Harvin, J. 2006, AJ, 132, 866
Riaz, B., Lodieu, N., Goodwin, S., Stamatellos, D., & Thompson, M. 2012, MNRAS, 420, 2497
Röser, S., Demleitner, M., & Schilbach, E. 2010, AJ, 139, 2440
Ségransan, D., Delfosse, X., Forveille, T., et al. 2000, A&A, 364, 665
Seymour, D. M., Mason, B. D., Hartkopf, W. I., & Wycoff, G. L. 2002, AJ, 123, 1023
Sicilia-Aguilar, A., Merín, B., Hormuth, F., et al. 2008, ApJ, 673, 382
Shatsky, N., & Tokovinin, A. 2002, A&A, 382, 92
Shkolnik, E., Hebb, L., Liu, M., Reid, N., & Cameron, A. C. 2010, ApJ, 716, 1522
Skrutskie, M. F., Cutri, R. M., Stiening, R., et al. 2006, AJ, 131, 1163
Smart, K. J., Ioannidis, G., Jones, H. R. A., Bucciarelli, B., & Lattanzi, M. G. 2010, A&A, 511, 30
Stassun, K. G., Mathieu, R. D., Mazeh, T., & Vrba, F. J. 1999, AJ, 117, 2941
Strigachev, A., & Lampens, P. 2004, A&A, 422, 1023
Thies, I., & Kroupa, P. 2007, ApJ, 671, 767
Tokovinin, A., Thomas, S., Sterzik, M., & Udry, S. 2006, A&A, 450, 681
Torres, G., Neuhäuser, R., & Guenther, E. 2002, AJ, 123, 1701
Tubbs, R. N., Baldwin, J. E., Mackay, C. D., & Cox, G. C. 2002, A&A, 387, 21
van Altena, W. F., Lee, J. T., & Hoffleit, E. D. (ed.) 1995, The General Catalog of Trigonometric Stellar Parallaxes (New Haven, CT: Yale Univ. Observatory)
van der Marel, R. P., Gerssen, J., Guhathakurta, P., Peterson, R. C., & Gebhardt, K. 2002, AJ, 124, 3255
Vennes, S., Thorstensen, J. R., & Polomski, E. F. 1999, ApJ, 523, 386
Voges, W., Aschenbach, B., Boller, Th., et al. 1999, A&A, 349, 389
Webb, R. A., Zuckerman, B., Platais, I., et al. 1999, ApJ, 512, L63
Weis, E. 1991, AJ, 101, 1882
Zapatero Osorio, M. R., Lane, B. F., Pavlenko, Y., et al. 2004, ApJ, 615, 958
Zuckerman, B., Song, I., Bessell, M. S., & Webb, R. A. 2001, ApJ, 562, L87